Final Report

PUBLIC

Development of an AMR Eddy Current-Based Crack Detection Sensor for Live Inspection of Unpiggable Transmission Natural Gas Pipelines

PHMSA Contract Number: **DTPH56-15-T-00013**

Submitted by:

NYSEARCH/Northeast Gas Association

Principal Investigator

Daphne D'Zurko,

20 Waterview Boulevard, 4th Floor

Parsippany, NJ 07054

973-265-1900, ext. 214

973-263-0919 fax

www.nysearch.org

ddzurko@northeastgas.org

April 2019

PUBLIC

Table of Contents

TABLE OF FIGURES

TABLE OF TABLES

1. Executive Summary

The Explorer family of robotic pipeline inspection platforms have proven their ability to provide valuable access to and data on unpiggable pipeline segments. This currently includes high resolution Magnetic Flux Leakage (MFL) data for metal loss detection, mechanical damage data as well as internal video images. As a result of recent pipeline incidents though, there is a growing desire for the addition of crack data on pipelines. While crack data can be obtained for piggable pipelines, at the present time is no methodology to provide that data on unpiggable pipeline segments. As such, the feasibility and prototyping of an eddy current (EC) sensor-based method of crack detection using Anisotropic MagnetoResistive (AMR) sensors was performed by Radiation Monitoring Devices (RMD) of Watertown, MA. RMD's work (carried out in a previous phase that is not part of this work) concluded that an AMR EC sensor could be implemented aboard a Pipetel Explorer 8in robot to potentially detect axially aligned cracks in unpiggable pipelines.

The objective of this project was to implement this validated sensor aboard the 8in Explorer platform and replicate test results from the earlier phase in a real pipeline test setting. This involved the conceptual development, design, manufacturing, system integration and testing of a full circumference AMR EC sensor in a module format that is compatible with Explorer's 8in modular robot. In addition, data analysis capability was developed.

InvoDane Engineering (IE) of Toronto, Canada, the developer of the Explorer robots, and RMD cooperated to determine a mechanical arrangement that would allow the sensor suite to be mounted to the 8in Explorer robot. This resulted in 15 sensor units with 8 channels, each arrayed in a collapsible assembly that can provide both full coverage of the pipe wall during scanning as well as maneuverability matching the rest of the robot when collapsed. This allows the robot/sensor assembly to negotiate practically any feature/obstacle in a pipeline, except a plug valve.

InvoDane developed the signal processing hardware and software to collect the eddy current data and validated it against laboratory testing. Tests were performed on a collection of samples with the following findings:

- Small sized manufactured defects can be detected, if there is an associated stress field (from defect manufacturing technique) without a residual magnetic field.
- Medium sized defects, 40% depth and greater, can be detected without an associated stress field, if there is a residual magnetic field.
- Most defects in an unpressurized pipe sample with naturally occurring cracks in the seam weld could not be detected (may be related to change in stress field since crack formation under pressure, but not validated).
- Defect sizing was not possible at this stage due to the variance in output from sensor to sensor.

A live field trial was conducted in alive pipeline operated by one of the funding companies. The operation of the integrated robot/sensor system met all operational, mechanical, electrocin and formware specifications. Regarding defect detection, the data obtained during the field testing provided results similar to those during laboratory testing. Additional testing, carried out following the field testing, concluded that defects made without stress are not detectable before magnetization and not distinguishable from regular material variation anomalies with magnetization.

The project resulted in a setup that reliably produces data showing a combination of stress, magnetic and material properties of a pipe and is deployable in a live pipeline setting. Anomalies with residual stress and anomalies with the application of residual magnetic fields are detectable but could not be differentiated from each other and from the regular signals seen due to material properties variations.

2. Introduction

Since 2004 InvoDane Engineering (IE), NYSEARCH/Northeast Gas Association (NYSEARCH/NGA), and PHMSA/US Department of Transportation (with occasional collaboration with other organizations) have collaborated to complete the development of the Explorer family of robotics platforms and to commercialize the technology. Explorer is a robotic inspection tool (Explorer 8 shown in ***Figure 1***) designed to inspect unpiggable natural gas pipelines and is deployed through a pipeline hot-tap. These robots use MFL (magnetic flux leakage) sensors to measure metal loss in the pipe due to corrosion. Through this work, the technology has been demonstrated to be capable at inspecting pipe segments with unpiggable features such as plug valves and 90-deg mitered bends, under flow or no-flow conditions. In the past nine years, InvoDane and NGA have also partnered to develop additional sensing and operational capabilities in order to offer a wider range of unpiggable pipeline inspection services.

FIGURE 1: EXPLORER 8

The Explorer robots are untethered, remotely controlled, self-powered robots for the visual and inline inspection of natural gas pipelines under live pipeline conditions. The Explorer 8, Explorer 10/14, Explorer 16/18, Explorer 20/26 and Explorer 30/36 offer visual and high resolution magnetic flux leakage (MFL) sensing in addition to mechanical damage detection using an optical, laser-based, sensor.

The Explorer robots can navigate pipelines with a significant bore reduction of up to 75% of outer diameter and a maximum pressure of 750 psig. Pipeline features that these robots are able to navigate include vertical and inclines pipeline segments, short radius bends, mitered bends, tees and, in the case of the larger robots, valves. These robots are bi-directional and travel at a speed of up to 20 ft. per minute.

Inspections are performed under live pipeline conditions without the need of shutting down or reducing gas flow in the pipeline during the inspection. The robot is launched into and retrieved from a pipeline via a hot tap fitting (***Figure 2***). There is no need for any pre-built infrastructure, such as a trap, for launching and receiving. Explorer provides live video images of the pipeline and integrity data. Video imagery and integrity data acquired by the Explorer robots is analyzed by Pipetel's team of analysts, using proprietary software (Pipetel, a sister company of InvoDane, is the company providing the inspection services to the natural gas industry).

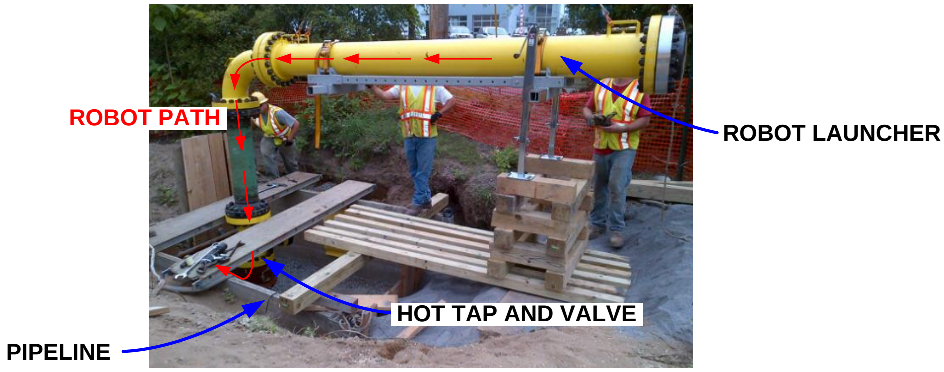

FIGURE 2: EXPLORER LAUNCH CHAMBER CONNECTED TO HOT TAP ON A LIVE PIPELINE

Recently, a number of high profile pipeline incidents have occurred that have caused the public and the industry to call for reviews and revisions to pipeline integrity regulations in the US. This has led to a push for increased inspection of unpiggable pipelines and a desire for the addition of crack detection technologies to the Explorer family of inspection robots. The Explorer family provides metal loss detection for unpiggable pipelines through MFL technology, but not crack detection as is currently available with standard inline inspections that use smart pigs.

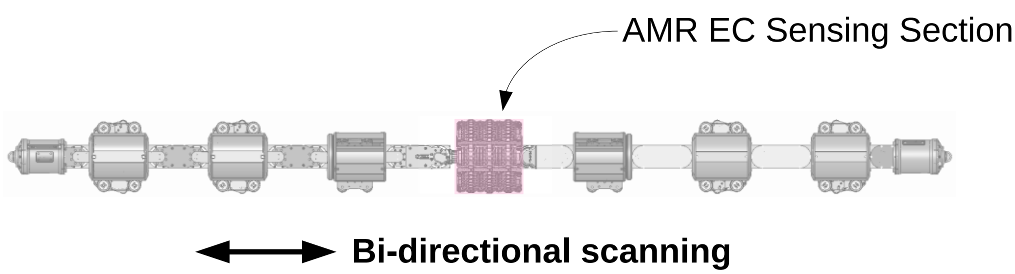

FIGURE 3: EXPLORER WITH AMR EC SECTION

An eddy current (EC) based method of crack detection using Anisotropic MagnetoResistive (AMR) Sensors was the subject of feasibility and prototyping studies performed by Radiation Monitoring Devices (RMD) based in Watertown, MA. The studies concluded that an AMR EC sensor could be implemented aboard an Explorer 8in robot (***Figure 3***) to detect axially aligned cracks in pipelines. The objective of this project is to implement the sensor aboard the 8in Explorer and replicate test results from the first two phases in a real pipeline test setting. It is expected that the sensor is scalable, so that the same concept can be employed in other Explorer sizes in the future.

3. Approach

A collaborative effort between InvoDane and RMD was implemented to develop the technology. RMD had the primary responsibility for designing the sensors, while IE had the responsibility of designing the sensor module, integrate it on Explorer 8 (able to inspect 8in pipelines), and carry out the field testing program. The following tasks provide an outline of the effort in hand.

RMD TASKS

Task 1.1 Finalize design of sensor system. Perform engineering and testing required to meet the final specifications for integration of the sensors onto Explorer, prepare the needed documentation, and establish quality control procedures with InvoDane for defect detection operational procedures related to the sensors.

Task 1.2 Fabrication of (16) sensor modules. Sixteen sensor modules (eight for the Explorer sensor module and eight spare) based on final design specifications to be delivered to InvoDane for integration on Explorer. Quality control and burn-in tests performed.

Task 1.3 Sensors testing and delivery to InvoDane. The sixteen modules would be fully -tested and then delivered to InvoDane.

Task 1.4 Service and support to InvoDane. RMD would provide the necessary technical support to InvoDane during InvoDane's effort to integrate the sensors onto Explorer 8. In addition, RMD would support InvoDane during preparation and implementation of the field testing effort.

INVODANE ENGINEERING TASKS

Task 2.1 Sensor module concept development. Conduct a conceptual study of a collapsible sensor arrangement to accommodate full circumferential scanning coverage in an 8in pipe while maintaining the existing robots ability to navigate tight pipeline features. Analysis of sensor spacing and general architecture of the sampling, processing and storage occurred at this time.

Task 2.2 Detailed design. Prototype the sensor geometry. RMD to miniaturize the AMR EC sensor element coil driver and analog pre-amplifier to achieve the same results as the test samples generated. Pressure test the sensor components to confirm stability of the signal. Prototype and test the processor and analog conditioning electronics on the bench using the sensor components from the previous step. Completely conceptualize the overall sensor system at this time. Implement the first iterations of data analysis techniques during this step.

Task 2.3 Manufacturing of Explorer sensor module. Manufacture and assemble the sensor components. Pull test the system in a pipe with known defects to verify the response achieved in prior steps.

Task 2.4 System integration. Finally, integrate the sensor with the Explorer robot and collect and analyze data. Create procedures for quality data collection and presentation. Test integrated Explorer robot/sensor in the laboratory prior to a field trial in a live gas pipeline.

Task 2.5 Data analysis development. Source a number of test samples to test the detectability of the sensor element under different conditions. Perform parameter sweeps using a single element on the test setup. Include tests to determine the effect of sensor lift-off, driving current, frequency, magnetization, test material, speed of travel, and sensor element geometry. At the end of this step, test a single sensor in a pipe to view a typical response.

Task 2.6 Pipeline testing and additional laboratory testing. Deploy the robot in an underground field trial to ensure the system could be operated in normal pipeline conditions. Collect and analyze data according to the tools developed in the previous steps. Collect additional data samples from an expanded pipe defect set and analyze.

Task 2.7 Project management. Conduct project updates and communicate with various organizations on the progress and status tracking. Keep the project on pace and make necessary adjustment to the project plan as the project evolves.

Task 2.8 Processor Development (added later during project). The additional functionality of digital signal processing and data storage was added to the sensor module. Miniaturize the sensor element electronics so that a number of them could be arrayed to fit around the pipe circumference and provide full coverage (according to the concept). Eliminate any interference with between sensors, as well as interference with the rest of the robot.

This report contains the activities associated with each of these tasks.

4. Project Tasks

Tasks 1.1 to 1.4 were carried out by RMD. The reporting of that work is included here in **Appendix A.**

Tasks 2.1 to 2.8 were carried out by InvoDane. The reporting of that works follows here.

Task 2.1: Sensor Module Concept Development

Target Requirements

The defect type targeted for this sensor is primarily axially aligned cracks on both the inner diameter (ID) and outer diameter (OD) of the pipe wall. Also required are the detection of other weld defects such as mill flaws and some secondary defects including fatigue cracks, stress fractures, corrosion, pitting, and anything where there is a conductive discontinuity.

The sensor module needs to sample the pipe while continuously moving parallel to the pipe axis, thus mapping out the pipeline surface as the robot moves through the pipe. Most inspections will operate with the robot moving in a forward motion from points A to B within a pipe. While reversal of movement and inspection in both directions is possible, it is desired to scan in one pass for operational efficiency.

The sensor module needs the ability to collapse to the same envelope as the current MFL sensing section with connection points at each end of the envelope for power and communication. This is to match the existing robot requirements for launching and navigating tight features.

Technology Background

The sensor intended for integration with Explorer for crack detection is based on an eddy current generation and detection methodology. These sensors typically use at least one coil with an alternating current to generate eddy currents in the material. The material response changes in the vicinity of discontinuities and this can be recorded by closely analyzing the phase and amplitude of the drive coil current or a sensing coil. This is a standard and well-known method of non-destructive testing and is very sensitive to surface conditions and variation in lift-off (the distance between the sensor and the surface of the pipe). A modification of this technique was proposed by RMD, the supplier of the sensor. In this technique, the sensing coil is replaced with an AMR (Anisotropic MagnetoResistive) sensor. The sensor detects variations in the magnetic field above the surface of the material that are perpendicular to the pipe surface. These variations can be caused by the eddy currents responding to changes in material properties or defects or other conditions such as lift-off. The AMR sensors are also influenced by the direct coupling to the driving coils; however, this effect is constant per sensor.

In the earlier work, not part of this project, various configurations were tested on the location and size of the drive coil. An optimal configuration was developed that was integrated onto Explorer.

System Concept

The system to be designed and integrated onto Explorer consisted of the following components:

- **Sensor module:** Each sensor module incorporated the unique eddy current arrangement developed during the earlier work. These units were designed and built by RMD.
- **Sensor element software:** Each sensor requires conditioning, sampling, storage, and communication with the robot. This unit was designed and built by InvoDane for the project.
- **Centerbody:** The mechanical chassis that holds the system together and connects to the Explorer robot. This unit was designed and supplied by InvoDane.

Sensor Module

Overall, the element has the following components:

Coils: The coils are wound on a curved surface designed to match the average curvature of an 8in pipe (Standard Schedule).

Coil driver: The coil driver amplifies a supplied waveform into the element. The coil driver operates so that it minimizes power consumption.

AMR Sensors: Multiple AMR sensors are located on each element. The sensors are mounted on a curved profile.

Sensor Pre-amp: Each AMR sensor output is pre-amplified before being sent to the signal conditioning board.

Signal conditioning: Each sensor’s output is conditioned further with a high-order low-pass filter and an amplifier with a processor controlled gain.

Processor: The DSP (Digital Signal Processor) runs a lock-in amplifier on each channel. The processor samples each channel simultaneously, and outputs the proper values. The processor also communicates to the rest of the robot via standard communication protocols.

Flash memory: The processor records values to non-volatile storage at the same rate as the entire robot for download after the scan. Each element has storage capacity corresponding to two full days of data collection.

The functionality described above is packaged into a single element, of which there are 15. The coils are secured to a nylon base and epoxied into place. The leads of the coils are soldered directly to the coil amplifier. The AMR sensors are soldered to the sensor conditioning board on a jig to ensure proper spacing. The two boards are then mounted to the nylon base.

The remaining boards sample, process, and store the data from the AMR sensors. The development is described in Task 2.8. These are mounted on spacers to the nylon base. Last, a nylon cover ensures the entire element is free from dust ingress. Nylon is used so as not to interfere with the EC field or data collection, as it is electrically non-conducting.

Overall power consumption for the entire system is higher than originally anticipated and is driven by the processor power as well as the analog conditioning components.

Centerbody

The system concept is described in *Figure* . A chassis is built to hold three rows of five AMR EC elements each. These elements are connected to power and communication through two adjacent steer control modules (Steers). These are the same steer control modules that exist on the current Explorer robot, modified to communicate with the new sensor module. The steers also connect the centerbody actuator to a shaft position counter to determine the diameter that the centerbody is expanded to ensuring contact with the wall of the pipe during scanning.

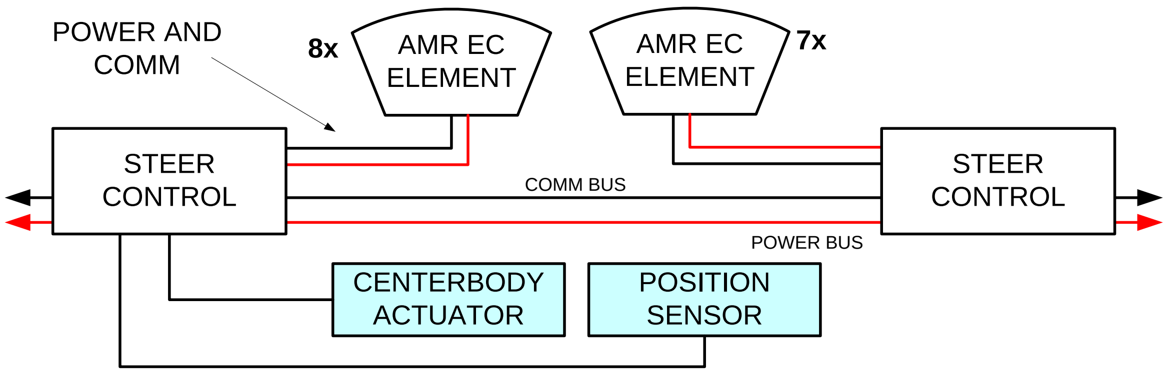

FIGURE 4: AMR EC SENSOR LAYOUT

The sensor elements are arranged in rows that are designed to expand and contract. Each element row is connected via the same flexible link. The positions of the sensors on each element have been selected to provide overlap when fully extended. This ensures that the full circumference of the pipe will be covered through one pass of the entire sensing section. The sensors ride on pads that provide a consistent spacing between the element and the pipe wall. Because of the flexibility designed into the sensor module, it will conform to local variation in pipeline diameter.

The centerbody has actuators at each end that connect to the rest of the robot. A third deploys and collapses the entire flexible array. The actuator can collapse the elements down to 75% of the pipeline diameter. The spring system extends the elements back to 100%.

The main power and communications bus for the robot passes through the AMR EC sensor module. The buses feed the steer control on both ends of the sensing section. Secondary communication and power cables feed each sensor element directly from the steer modules. Therefore, any failure of the sensing section will not affect the overall operation of the robot.

Additional software has been adapted from standard libraries aboard the steer controllers to operate actuators and read position sensors. The controllers provide the following functionality:

- Pitch and centerbody actuation and position
- Data download
- Secondary communication and power control

Task 2.8: Processor Development

This task was added to the workscope during the project to address the need for onboard signal processing (the results of this task are presented here out of sequence, given that they ultimately affected the final design of the rest of the sensor module). Additional hardware was designed to process the signal from the AMR sensors, provide the necessary power, and store the data. These were designed to perform a lock-in amplifier function, storage and communication with the robot.

Each element contains a digital signal processor that samples the output of the AMR sensors and performs a lock-in amplifying process to the each input simultaneously.

Task 2.2: Detailed Design

The detailed design was carried out on the sensor modules, software and centerbody to construct a prototype to be implemented aboard the Explorer 8 robot. During the design process, various system components were tested to verify functionality before incorporating into the final design. This includes the following tests:

- **Pressure testing**: to verify functionality and any deviation of performance due to external gas pressure.
- **Detectability testing:** to verify the ability of the sensor to detect axially aligned cracks and slots in steel. Magnetism may affect the threshold of detection.
- **Repeatability testing:** to verify the ability of the sensor channels to provide the same result on successive scans as well as the same result as each other.
- **Mechanical testing:** to verify the system performance under various pipeline scenarios such as pulling or deploying to the pipe wall.
- **Interference testing:** to verify that all sensor elements function independently, not interfering with each other and rejecting external noise.

Mechanical Chassis

The mechanical components that needed to be designed and implemented were the sensors and the centerbody chassis. Sensor components are mounted on spacers to the nylon base. A nylon cover ensures the entire element is free from dust ingress. Nylon is used so as not to interfere with the eddy current field or data collection.

The sensor element electronics were miniaturized so that a number of them could be arrayed to fit around the pipe circumference and provide full coverage (according to the concept). Any interference with each other was eliminated, as well as interference with the rest of the robot.

On the processing board, digital processing software was implemented to sample and store the AMR data.

A centerbody chassis prototype was constructed to test the actuation and control of the mechanical components. The following tests were performed:

- Collapsing and extension tests to ensure uniformity of extension to the pipe wall as well as the ability of the sensor section to reliably collapse down to the minimum diameter pipeline ID similar to the existing robot as required for launching and navigating tight pipeline features.
- Vibration tests to simulate any effects of vibration by rubbing a sensor on the pipe wall via a sliding sled.
- Pull tests to investigate the contact between the pipe wall and the sensors to ensure all sensors were correctly contacting the pipe wall. The pull links on each end were evaluated for strength.

Pressure Testing

Pressure testing is performed using nitrogen as a medium. The components are placed into a pressure vessel and electrical connections are passed through pressure rated connectors. The response of the system is monitored during pressurization, for a pre-determined duration at pressure (usually 1hr), and then again during depressurization.

The components in the sensor element were pressure tested up to 750 psig with the following observations made:

- No significant variations on signal magnitude or phase were observed
- Power consumption was stable in measurements taken before, during and after the pressurization.
- One coil showed variations due to deformation in a material used during winding that affected the inductance of the coil. This material was not used in the final implementation of the coil.
- Overall the coil driver and conditioning electronics were not affected by external pressure in the design testing.

Detectability Testing

Eddy current techniques require the use of a lock-in amplifier, which has two parameters as an output. These are the in-phase (I) and quadrature (Q) components of the signal with narrow frequency band.

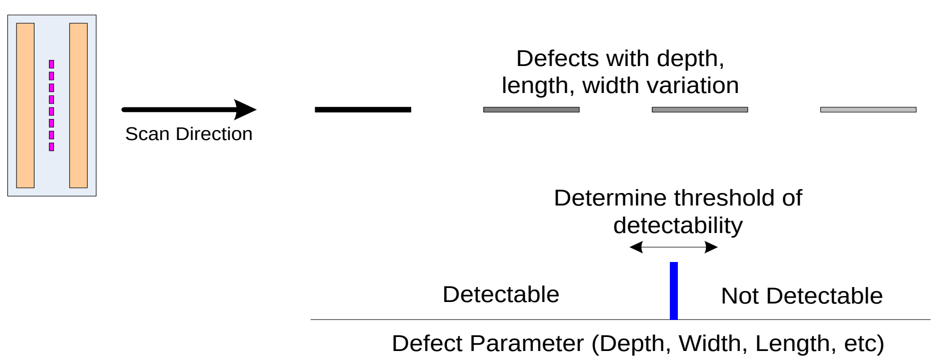

FIGURE 5: DETECTABILITY TESTING

The repeatability and detectability of the method for crack-like defects was studied (see Figure 5). The goal of the detectability testing was to replicate prior results with an in-pipe capable system and extend the measurements into sizing and more advanced data analysis techniques. In order to do this, tests were set up using flat plates and pipes with various characteristics (grade, thickness, etc.) and with various types of defects (machined slots, Electrical Discharge Machining slots, closed fatigue cracks, natural cracks, etc.). The test samples were scanned in the test rigs using the AMR sensor module in order to systematically determine the parameters that would be used for sizing in later stages of the project.

Test Setup

Detectability of cracks in pipes was tested using two different test rigs. First, because of ease of testing, a flat sensor was implemented to test defects in a flat steel plate (Figure 6). This is the same sensor as used in the repeatability testing. The second setup involved a curved sensor in an actual pipe with defects (*Figure 7*).

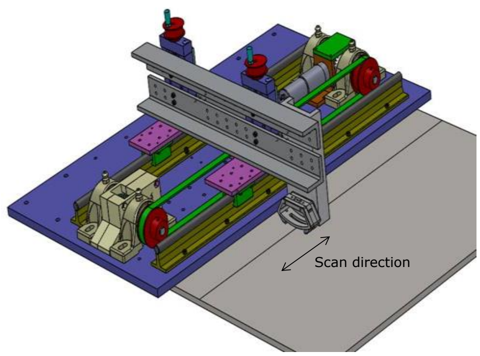

FIGURE 6: SENSOR TEST RIG FOR REPEATABILITY AND CALIBRATION

This rig was an intermediate step before the full sensor was integrated aboard the Explorer robot and gives an approximation of how the system would behave in a pipe. Between the two setups, the following scans were performed on the test defect set:

1) Control scans to determine the levels of variation in the material itself
2) Scans of machined and Electrical Discharge Machined (EDM) defects

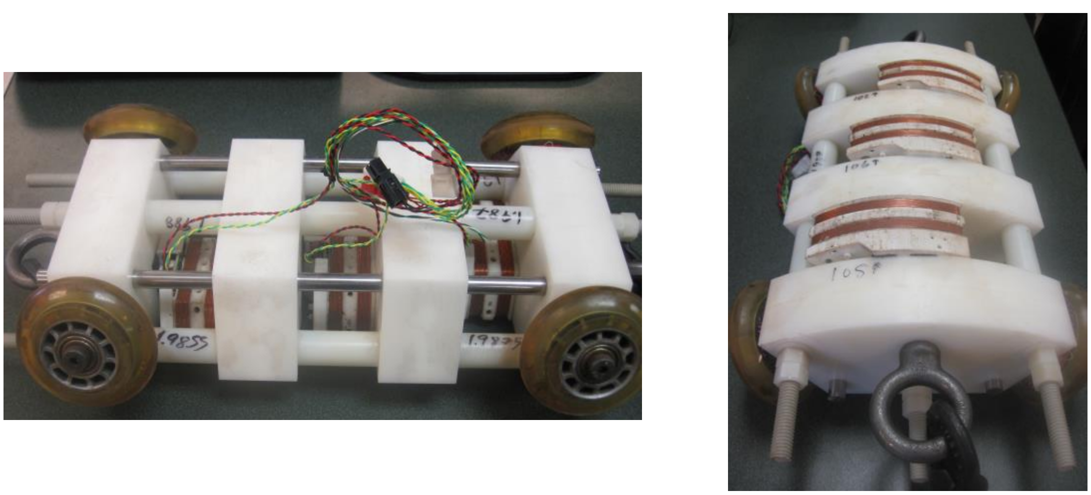

FIGURE 7: CURVED TEST SETUP

Defect Set

A defect set was sourced in order to facilitate measurement at every step of development, from single channel measurements to full scale module testing. The defect set, shown in Table 1, included variations in material (grade), surface type (pipe vs. plate), wall thickness, defect type (closed vs. open cracks), method of defect manufacture (EDM, machining, non-thermal fatigue, natural), and defect dimensions (width, length, depth).

TABLE 1: DEFECT SET SUMMARY

Sample	Material / Plate	Defect Type	Defects	Note
1	A36 / Plate	Machined slots	2	Base material
2	A36 / 0.250" Plate	EDM slots	2	Base material
3	A672 / 0.375" Plate	Non-thermal Fatigue	3	Base material
4	A672 / 0.250" Plate	Non-thermal Fatigue	3	Base material
5	A53B / ø8" 0.322WT Pipe	Non-thermal Fatigue	18	Weld and base material (Y)
6	A53B / ø8" 0.322WT Pipe	Machined slots	12	(X)
7	A53B / ø8" 0.322WT Pipe	EDM slots	9	
8	ø14" 0.250WT Pipe	Natural Cracks	50+	Cracks in seam weld
9	A53B / ø8" 0.322WT Pipe	EDM, non-thermal fatigue, thermal fatigue	4	
10	A53B / ø8" 0.322WT Pipe	EDM circular defects	16	

During testing it was theorized that the sensor would pick up a combination of residual stress, material variation, and residual magnetism in the material. Three techniques were employed to control these variations. To reset the magnetism in a material, a degaussing rig was used for both plates and pipes. Magnets were used to improve sensor response. Finally, some plates were thermally annealed to relieve stress in the material. Material variation was kept to a minimum by sourcing known steel grades.

In order to facilitate a known magnetic state of a sample, a method of degaussing plate or pipe samples was devised by wrapping the sample in magnet wire and connecting it to an AC power supply. If the entire surface of a plate is covered with the wound magnet wire, then reducing the AC power supply current from high to low will result in a degaussed plate. For a pipe, the coil wrap is moved from one end of the pipe to the other (*Figure 4* and *Figure*). With either of these methods, a specimen with unknown magnetic history can be effectively "reset" to a known, zero magnetic field condition.

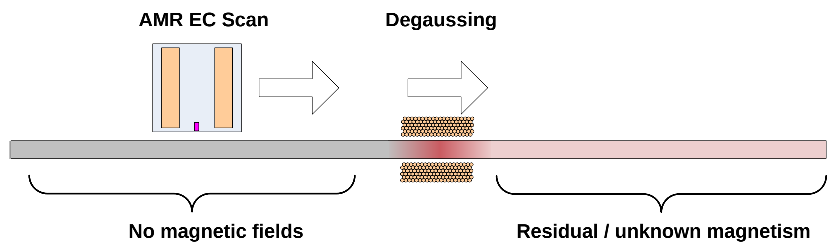

FIGURE 4: PIPE DEGAUSSING RIG

To re-magnetize a pipe or plate uniformly, strong magnets were used to leave a constant residual magnetic field in the sample. First, a magnet would be moved from one side of a plate to the other over the region of interest. This would leave a uniform residual magnetic field (Figure 10). This is a similar situation as an MFL sensor being used prior to an AMR EC run with a magnet being dragged through the pipe with a consistent field remaining behind.

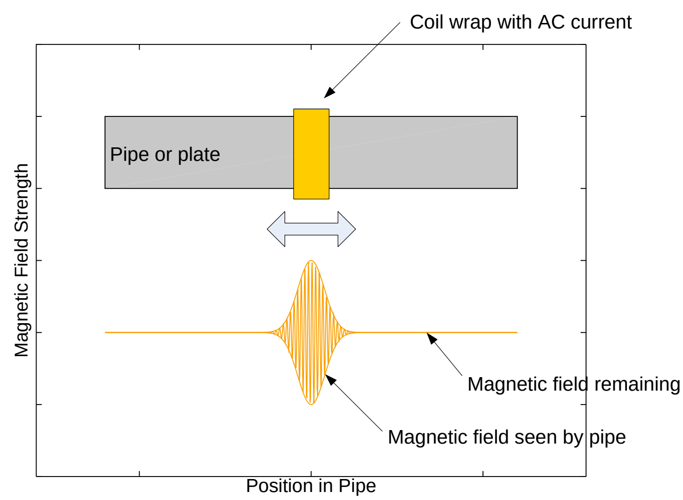

FIGURE 9: ELECTROMAGNET CURRENT FOR EACH DEGAUSSING PASS

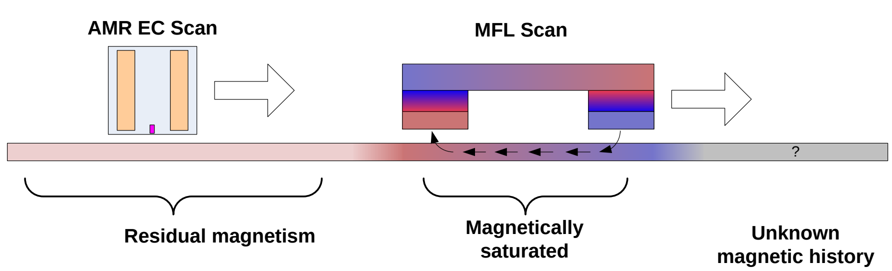

FIGURE 5: RESIDUAL MAGNETISM LEFT IN A PIPE AFTER AN MFL SCAN

Plate results

Several hot rolled A36 steel plates (0.250" and 0.375" thick) were sourced and scanned prior to adding defects. The signature of one plate (0.250" thick) as scanned (at 2.6kHz) is shown in *Figure 6*. The scan shows regions of the plate that have high peaks and valleys. It was unclear whether the anomalies were caused by residual magnetism, stress, or material properties variation.

The plate was then notched with two 50% deep, 1/16" wide, 1.5" long EDM (Electrical Discharge Machining) defects on the far side of the plate. This type of machining leaves little residual stress in the material. The scan was repeated to show the same noise levels as previously measured, with some additional regions of interest (see *Figure 7* for details).

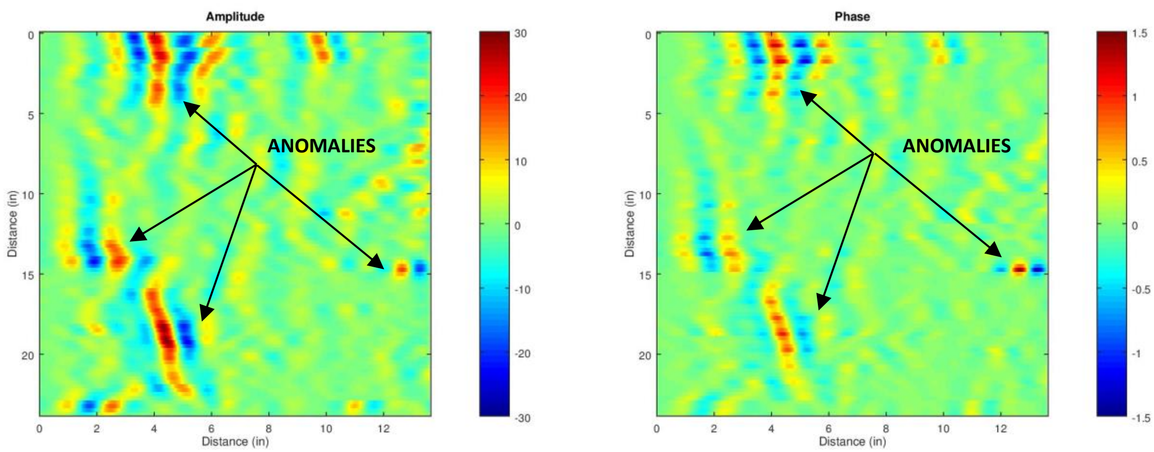

FIGURE 6: PLATE SCAN NO DEFECTS

The two regions where the defects were placed showed a weak signal response (actual flaws are slightly higher than marked on the plot). However, there were other sections of the plate that show new anomalies. From discussions with the vendor, these are regions where the plate was clamped in order to machine the defects (see *Figure 7* for amplitude and phase plots).

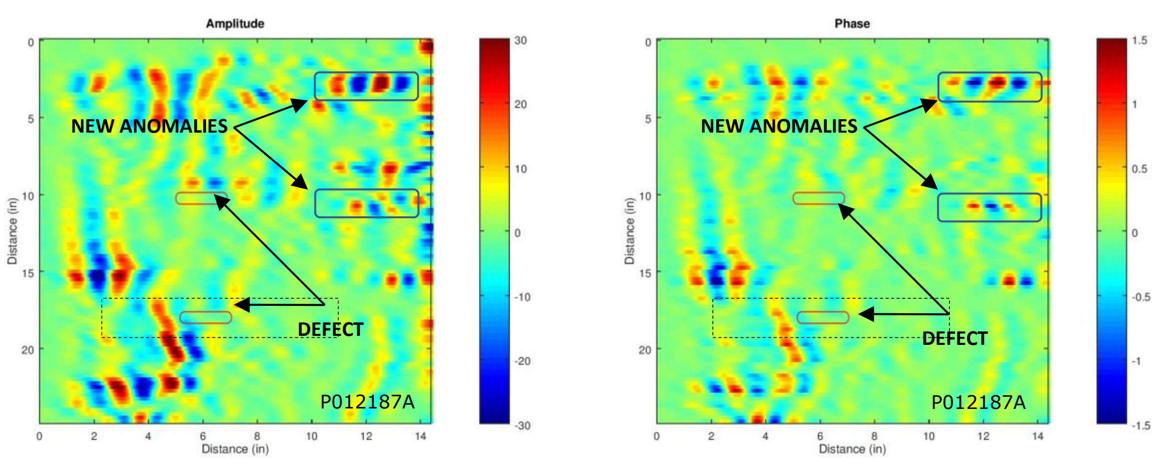

FIGURE 7: PLATE SCAN WITH EDM DEFECTS

The plate was then magnetized in a random fashion by moving a permanent magnet over its surface. The scan was re-performed a third time. One 50% defect shows up clearly on the plate while the other is not as easily identified, but can be seen (*Figure 8*). This shows that magnetizing the plate prior to scanning with the AMR EC sensing elements can both improve the signal magnitude as well as reduce the overall noise.

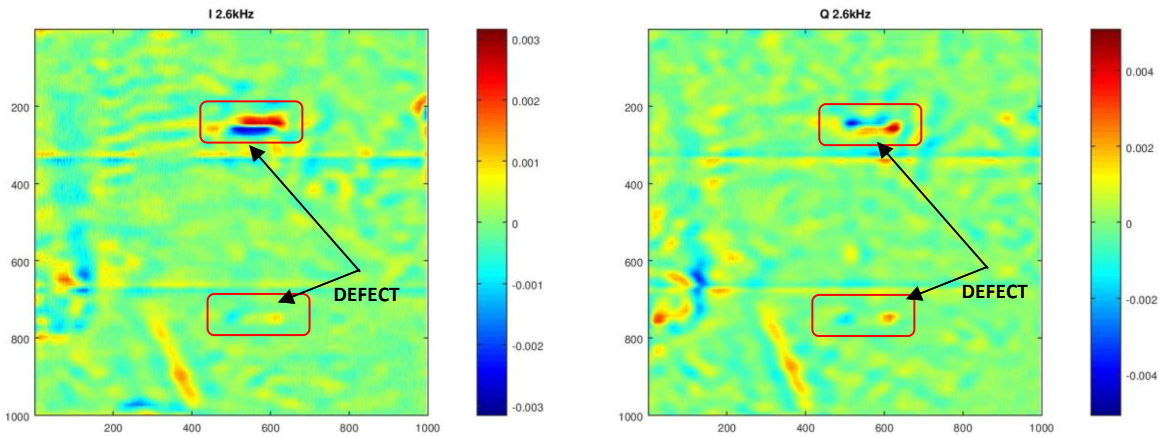

FIGURE 8: PLATE SCAN WITH EDM DEFECTS AFTER MAGNETIZATION

It is unclear whether the magnetization of the material increases the sensitivity of the response in the sensor itself due to the asymmetrical effect of magnetism on the sensor or if the magnetic field is varied around the defects themselves. As can be seen *Figure 9*, the sensitivity of the AMR sensor can change by -30% to +100% depending on the applied residual magnetism (applied DC field).

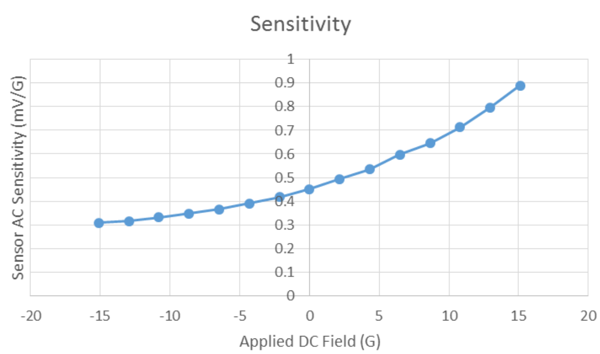

FIGURE 9: SENSITIVITY OF THE AMR SENSOR WITH APPLIED DC MAGNETIC FIELD

A second plate was sourced with three non-thermal fatigue cracks from 13% to 35% depth (1in long). These cracks were manufactured and measured after production to confirm accuracy of depth. Initial results showed that the cracks were visible. The plate was degaussed using the setup described in a previous section. Scans after degaussing showed a diminished response from the AMR scan. The plate was magnetized using a magnet bar pulled back and forth along the surface of the plate. The signals were evident in a similar fashion as the initial results. Therefore, adding the magnetization aided in identifying the simulated cracks.

Annealing the plate (relieving the internal stresses in the material) eliminated the ability to detect the cracks in this plate. In summary (shown in Table 2), for flat plate scans, EDM defects were not detectable unless the material was magnetized prior to scanning. Non-thermal fatigue cracks were detectable before and after magnetization. No defects were detected after annealing and degaussing a sample.

TABLE 2: PLATE SAMPLES RESULTS

Defect plates, various types of defects				
Sample	**Defect Type**	**Magnetism state**	**Detected defects?**	**Other**
Plate				
1	Machined slots	None	Yes	
2	EDM notches	None	No	Regions of interest in material,
2	EDM notches	Random	Yes	Regions of interest in material
3 and 4	Non-thermal Fatigue	Unknown	Yes	
3 and 4	Non-thermal Fatigue	Random	Yes	
3 and 4	Non-thermal Fatigue	None	No	Stress relieved by annealing

Pipe results – Simulated Defects

An 8in, 0.322in wall thickness (WT) A 53B line pipe was sourced and cut into two 10ft sections. The first section was sent to a 3rd party for non-thermal fatigue cracks to be manufactured. The second section was used in our lab to test the overall detectability of machined slots. First, the pipe was scanned with a single sensor element (8 channels) before machining slots in the pipe. The results are shown below in *Figure 10*. The results show various locations with relatively high peaks and valleys. It is assumed that these anomalies are a direct result of the pipe manufacturing process. Some anomalies look very similar to the signature of the defects observed from the plate tests for detectability and repeatability.

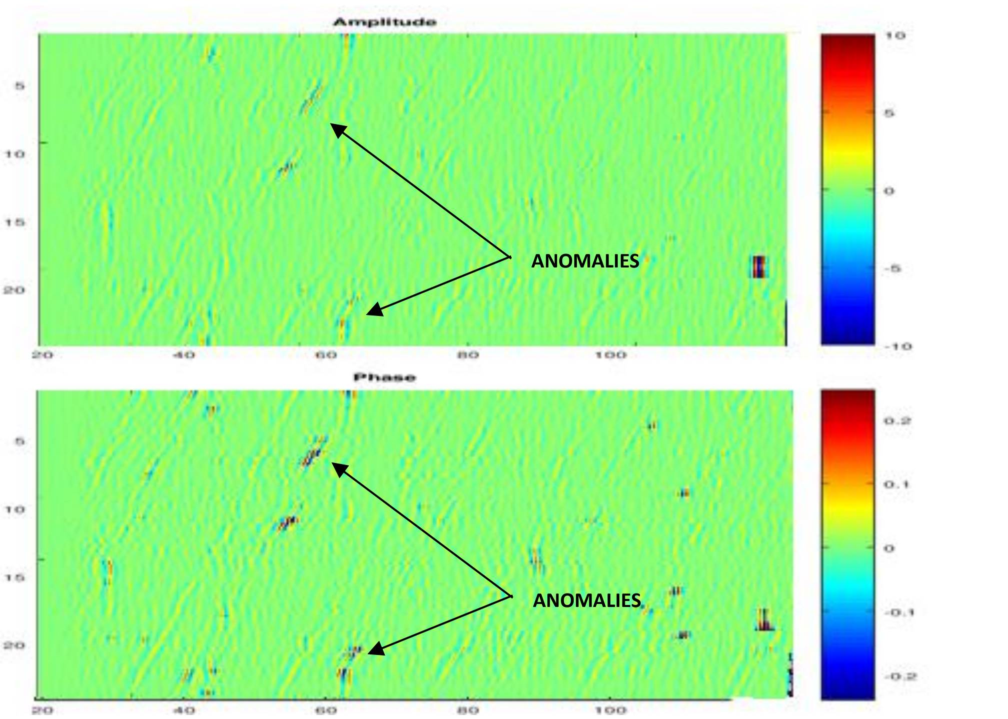

FIGURE 10: 8IN PIPE NO DEFECTS

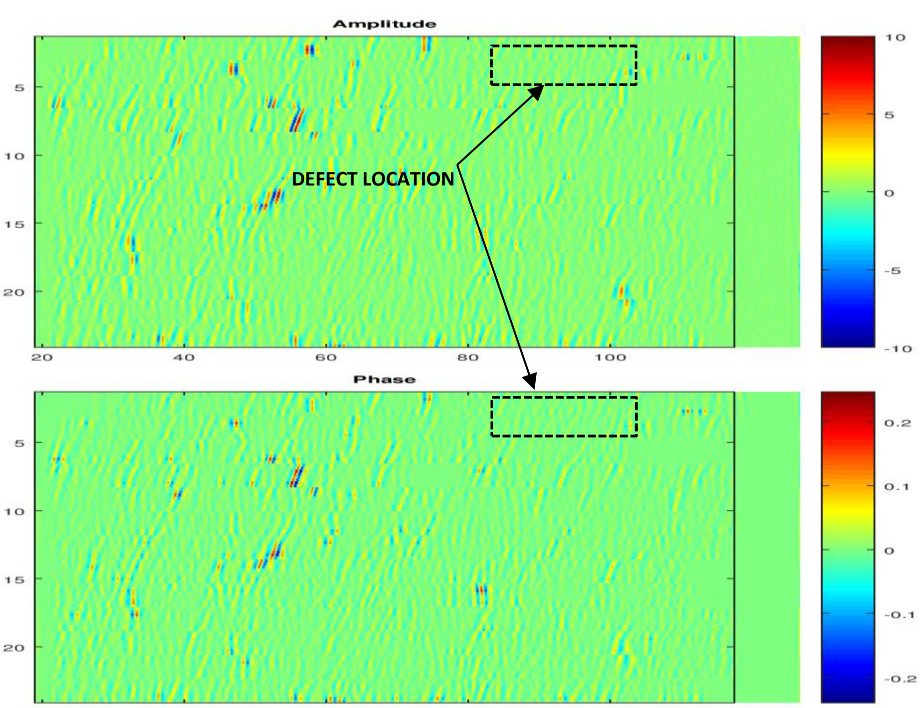

FIGURE 11: 8IN PIPE WITH DEFECTS

Two 1 inch long defects were machined into the pipe OD, at 30% and 50% depth, 1/8in wide. The whole pipe was scanned again using a single 8 channel element. The results are shown in *Figure 11*. While there may be some indication that the defects are present, the signal magnitude and phase are similar to the overall noise in the pipe from the control scan.

As mentioned in the previous section, it was found that by magnetizing the material prior to scanning the noise patterns were diminished relative to the signatures of the defects. To show this result in a pipe, an MFL sensing section was run through the pipe starting from the right hand side. The magnetizer was switched off halfway through the pipe. The resulting effect can be seen in *Figure*. On the left side is the non-magnetized portion of an 8in pipe, 0.322in WT.

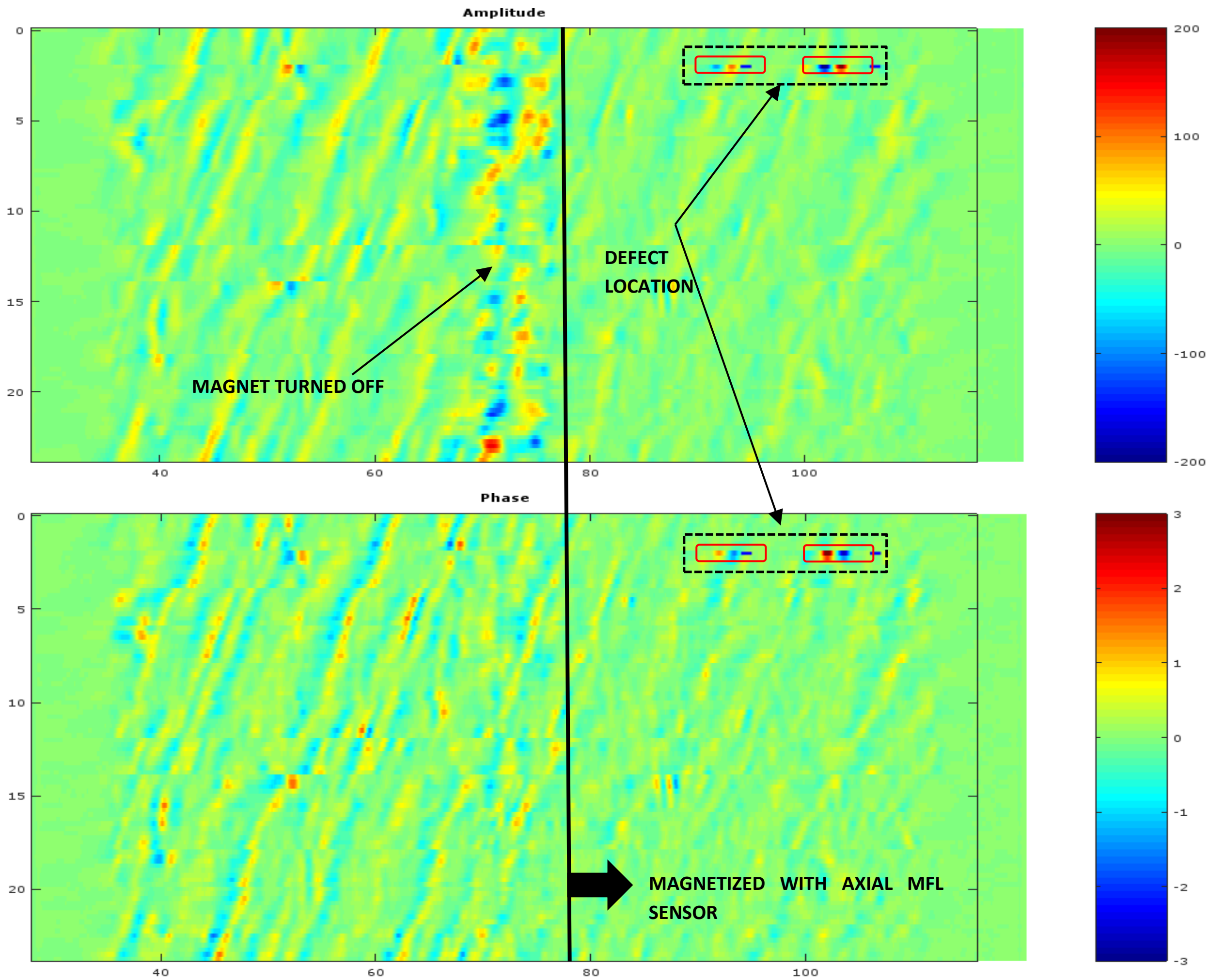

FIGURE 17: MAGNETIZATION EFFECT ON EDDY CURRENT SIGNALS

The ridges and valleys of the material magnetic properties can be seen. In the middle of the graphic, there are distinct signatures of residual magnetism where the magnets were turned on and off. On the right hand side, the two defects, 30% and 50% are plainly seen where they are barely visible in the previous scan. Furthermore, the overall noise from the pipe material itself is diminished in the magnetized section. This test points towards the usefulness of magnetizing the pipe prior to scanning with the eddy current sensor.

Defects were machined in the same pipe from 10%-100% (thru) deep. The pipe was degaussed in order to neutralize the magnetic state of the pipe. The pipe was scanned again and the results are shown in *Figure*. The machined defects can be seen in the data (I component) from 50% to 100%. This shows that for machined defects, without magnetism, the sensor is picking up a signature from the defects.

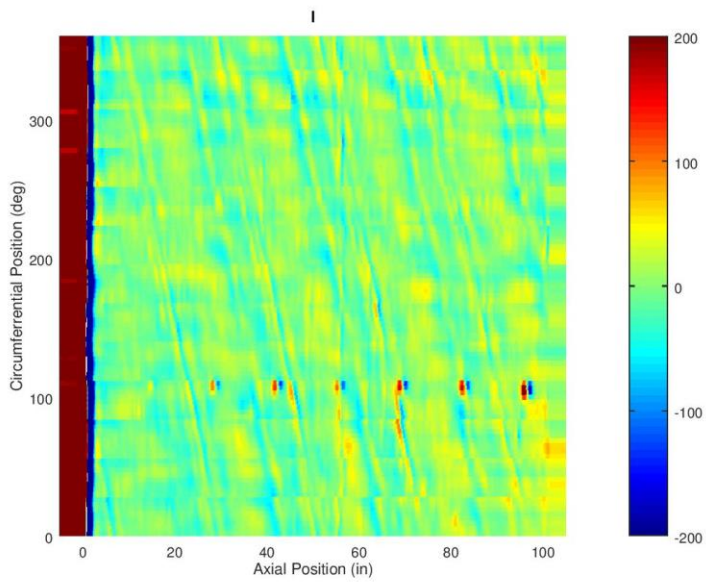

FIGURE 18: MACHINED DEFECTS IN 8IN PIPE

Finally, a pipe with non-thermal fatigue cracks was sourced. The defects were manufactured by local cycles of a stress to create the defect. Defects were measured after manufacture by phased-array ultrasonic techniques to verify depth and length. A total of 21 cracks were put into the test pipe in various locations. Crack lengths varied from 0.25in to 2in, depths ranged from 10%-50%. Five defects were placed directly on the seam weld while the rest were placed elsewhere in random locations.

In agreement with prior phases, all defects were detectable using the AMR Eddy current sensors (non-magnetized state shown in *Figure 19*). However, it was questioned whether it was realistic that the sensor should be able to detect a 10% OD defect, as it was unable to detect a 40% OD machined defect. Reviewing the manufacturing method with the vendor, it was confirmed that the technique used to generate the defect would result in residual stress / grain structure changes in the material. This technique has been used in prior samples used to determine the viability of the sensor.

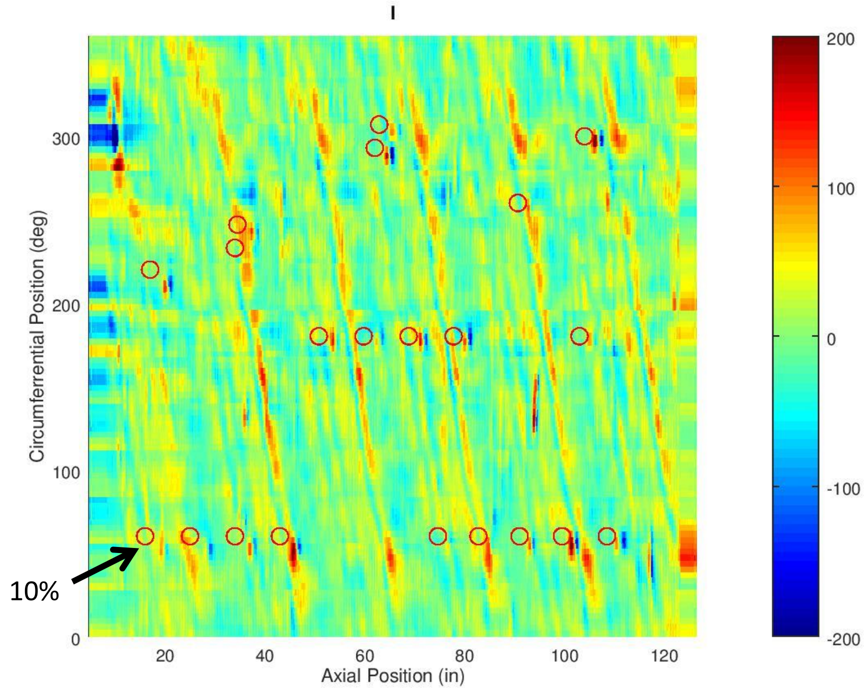

FIGURE 19: NON-THERMAL FATIGUE DEFECTS IN 8IN PIPE

In summary (results shown in Table 3), for 8in pipe with machined or simulated defects, all simulated defects and deep machined notches can be detected with the AMR sensor. It seems as though the presence of a stress field due to the manufacturing technique causes the defect to become detectable. For shallower defects, magnetizing the pipe causes shallower defects to be distinguishable above the noise floor. This is a similar behavior to the plate tests performed in the previous section.

TABLE 3: PIPE SAMPLES RESULTS

8in A53B 0.322" WT pipe, machined and simulated defects				
Sample	**Defect Type**	**Magnetism state**	**Detected defects?**	**Other**
5	None	None	No	Regions of interest in material
5	Machined notches	None	Yes	50% depth and greater
5	Machined notches	Axial	Yes	30% and 50%
6	Non-thermal Fatigue	None	Yes	Detected all defects (10%-50%)
6	Non-thermal Fatigue	Axial	Yes	Detected all defects (10%-50%)

Pipe results – Naturally Occurring Defects

The Northeast Gas Association in partnership with Battelle Memorial Institute located two pipes[1] with naturally occurring cracks in the long seam weld. These pipes were 14in diameter, and 40ft and 24ft long respectively with a wall thickness of 0.250 in. The pipes had been manufactured circa 1941 by Republic

[1] Pipe provided by Battelle Memorial Institute, originally collected under DOT Contract DTPH56-11-T-000003L

Steel. The pipes had been the subject of a research study by Battelle to understand longitudinal ERW seam failures. The seam welds had been characterized using a variety of ultrasonic methods included Phased Array Ultrasonic Testing (PAUT) and Inverse Wavefield Extrapolation (IWEX). The methodology and results of these testing techniques are not discussed in this report. There were a total of 15 defects in the first pipe (14-03) that were 25% or greater and were surfacing (ID or OD) and 5 defects that were greater than 25% and non-surfacing. The second pipe (14-04) had one surfacing flaw.

Both pipes were scanned using the curved scanning rig (three AMR EC sensor modules). The rig was moved back and forth using a motor / pulley system attached to each end of the pipe (*Figure*). Initial scans (*Figure 12*) show higher background noise than pipe sourced for simulated defects (previous section). The pipe was degaussed using the same technique but that did not have the same effect as in previous cases. The background noise was not reduced to the same extent as previous uses. Of the 20 defects in the seam weld, three were identified using the AMR EC sensor (*Figure 13*).

Cleaning pipe prior to scan

Degaussing Pipe

Scanning with curved rig

FIGURE 20: BATTELLE PIPE TESTING PHOTOS

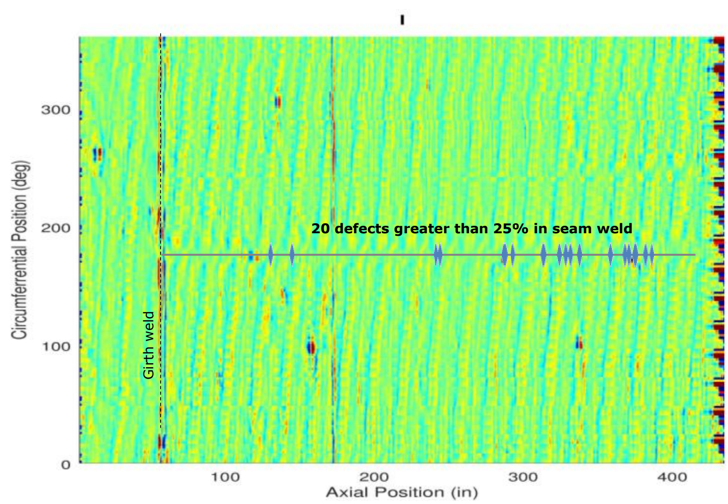

FIGURE 12: LOCATION NATURAL CRACKS ON SEAM WELD

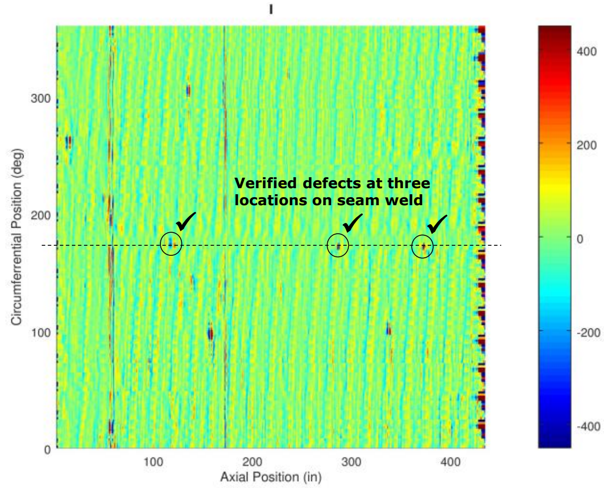

FIGURE 13: THREE VERIFIED NATURAL CRACKS ON THE WELD

A phased array ultrasonic transducer (PAUT) scan was performed on the pipe with confirmation that there were anomalies in the material at three locations on the seam weld. The depth and length of these defects could not be measured without calibration and was not pursued due to time constraints with the test sample. Efforts to measure the full pipe using phased array were unsuccessful. Table 4 summarizes the results of these tests.

TABLE 4: NATURAL CRACK SAMPLES RESULTS

Sample 8, 14in pipe (ERW) with naturally occurring cracks Pipe			
Defect Type	**Magnetism state**	**Detected defects?**	**Other**
Natural cracks	None	No	Higher background noise
Natural cracks	Axial	No	Noise isn't reduced like in 8in pipes, some indications but less than 10% of existing cracks

Detectability summary

The AMR sensor seems to be sensitive to changes in the material (background scans) and local changes in magnetic fields (machined slots, fatigue cracks, residual magnetism). There are two cases that are troublesome for detection of cracks. First, the pipes of unknown magnetic history, cracks and material variation look very similar when viewed in data analysis. Second, for pipes with known magnetic history (either through degaussing or MFL scanning), simulated defects are always detected, but naturally occurring ones are not.

Repeatability

The goal of this series of tests was to determine if the same result could be recorded by adjacent sensors and modules on a consistent basis. There are three types of repeatability scans that needed to be performed in order to establish an approach for sizing (*Figure 14*). First, each channel would need to provide the same result for repeated scans. The test for this is to take a sensor and repeatedly scan the same defect. Each measurement should result in the same signal response. Second, each channel will need to provide the same result as each other. The test to establish channel-channel repeatability is to repeat the first test with a different channel and compare the two sets of data. Third, from module to module, each sensor needs to provide the same result, regardless of its position next to other modules. The test to establish module-module repeatability is to replace modules in the first two tests.

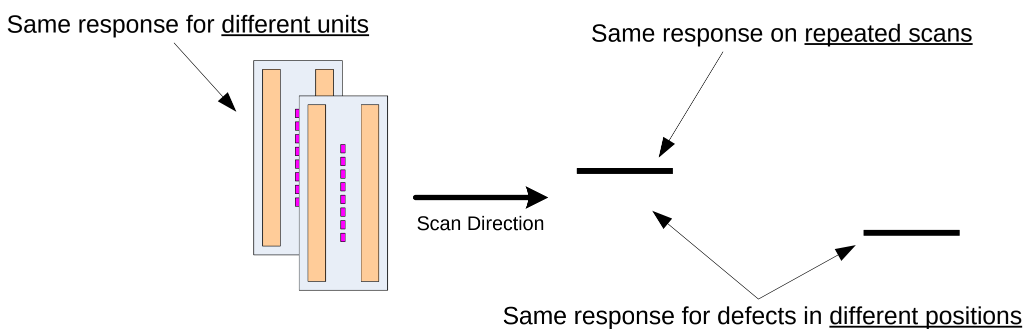

FIGURE 14: REPEATABILITY TESTS APPROACH

It is not realistic to move forward with channel-channel repeatability, if each channel does not provide repeatable results. Similarly, it is not realistic to expect module-module repeatability if channel-channel repeatability does not exist.

Single channel repeatability

Single channel repeatability was performed early in the development cycle using a laboratory lock-in amplifier to measure the phase and magnitude of AMR signal. A single channel AMR sensor positioned in a similar curved exciter coil was moved along a straight line on a plate with closed cracks. The sensor was moved left to right (L-R) and then right to left (R-L). The phase and magnitude was measured for each pass with the difference between the two passes less than 1% of for both parameters (*Figure 15*).

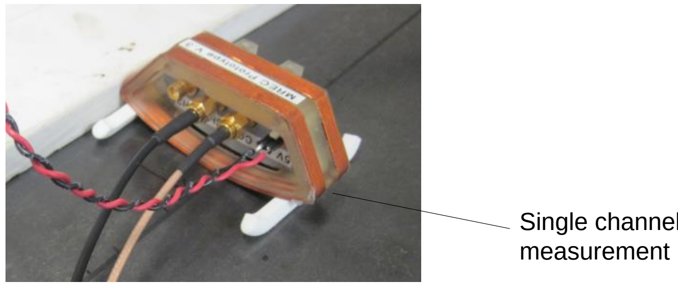

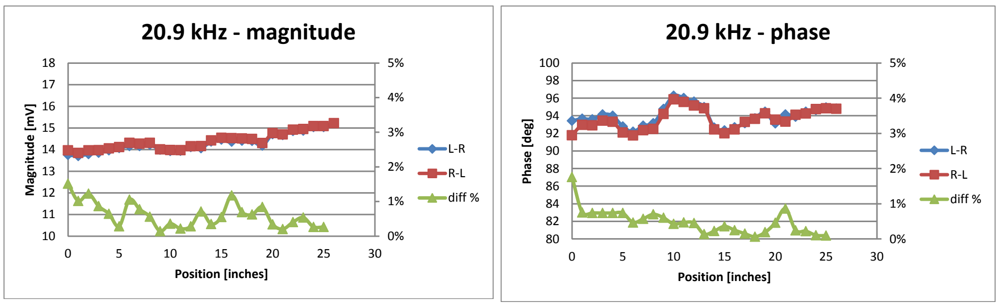

FIGURE 15: AMR SINGLE CHANNEL REPEATABILITY

<u>Channel-Channel Repeatability</u>

Channel-channel repeatability scans were performed by taking a scan of defects on a plate and then shifting the element and re-scanning the same defects. The test setup used was the same as in the detectability tests. The test sample used was the machined slot plate. Data from two channels were measured using the AMR EC module. The sensor was moved from end to end 8 times shifted by the width of the sensors. The rig used to perform this is shown in *Figure* and *Figure 16*.

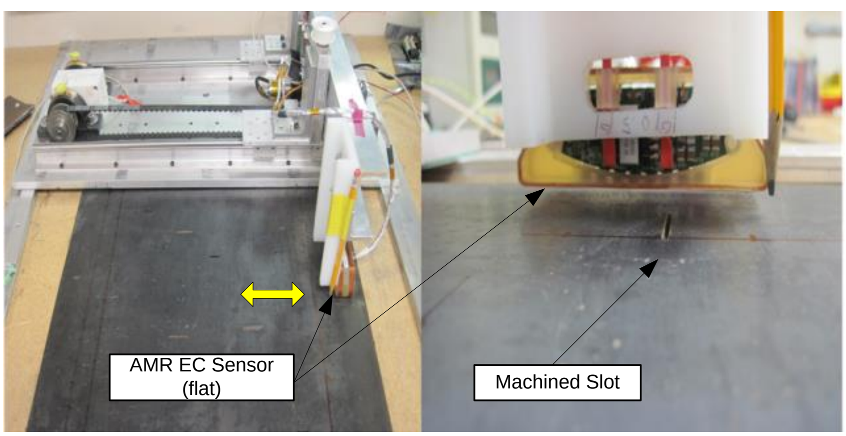

FIGURE 16: AMR CHANNEL-CHANNEL REPEATABILITY TEST

The results of this sensor repeatability test showed a difference between the responses of adjacent sensors to the same physical feature. This behavior is shown in *Figure 26* and 27. The graphs show response of two different sensors. The behavior is similar (the defect is detectable) but the scale is different. This data shows that the sensors do not appear to have the same response when passed over the same location on the material.

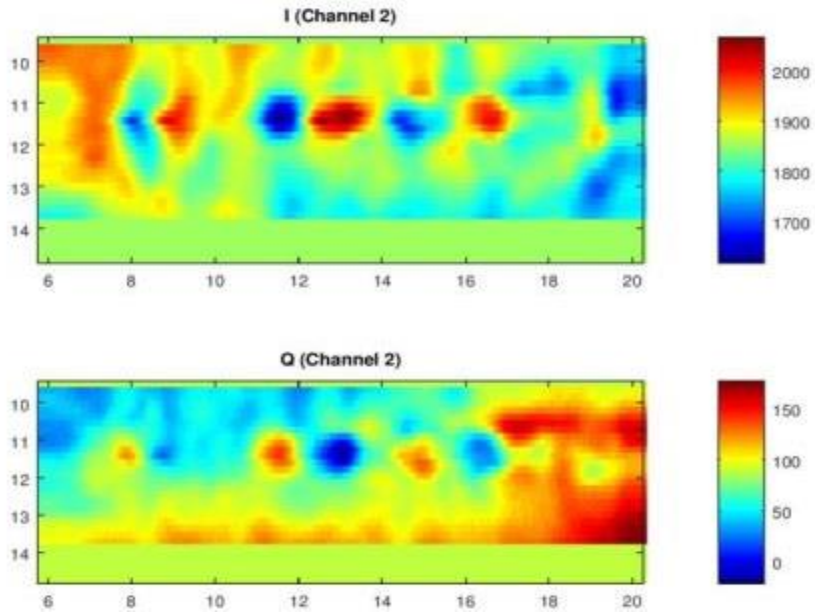

FIGURE 26: DEFECT RESPONSE BY CHANNEL A

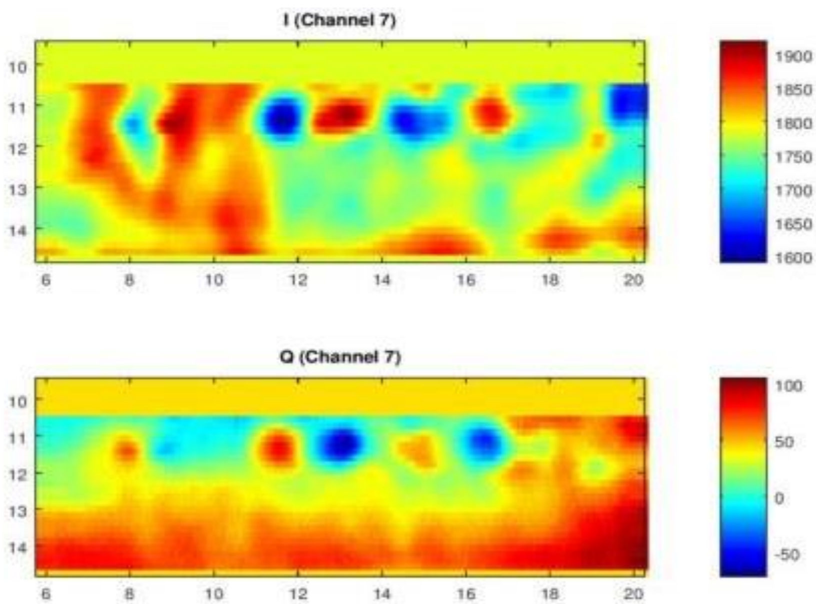

FIGURE 27: DEFECT RESPONSE BY CHANNEL B

Based on these results, it was determined that the sensor will need to be calibrated before we are able to determine the detectability specification and eventually move into developing sizing algorithms. Calibration development was performed by the sensor provider. It was found during this stage that the AMR sensor positioning on the module had variability, which caused changes in sensor output, so the sensors were potted in place with epoxy.

Note that InvoDane measurements of repeatability using miniaturized electronics were comparable to the RMD's results using a commercial lock-in amplifier, validating our signal conditioning and processing steps.

After the full AMR EC crack sensor was constructed (15 modules), these tests were repeated in a pipe with defects. The first repeatability test was done to ensure that results from the flat plate would be applicable to in-pipe measurement. First, the sensor was pulled through a pipe multiple times, over several days. It was found that the peak measurement on a set of defects varied significantly (Figure 28). Further, apart from the thru hole defect, there was no correlation on the peak values to the depth of the defect.

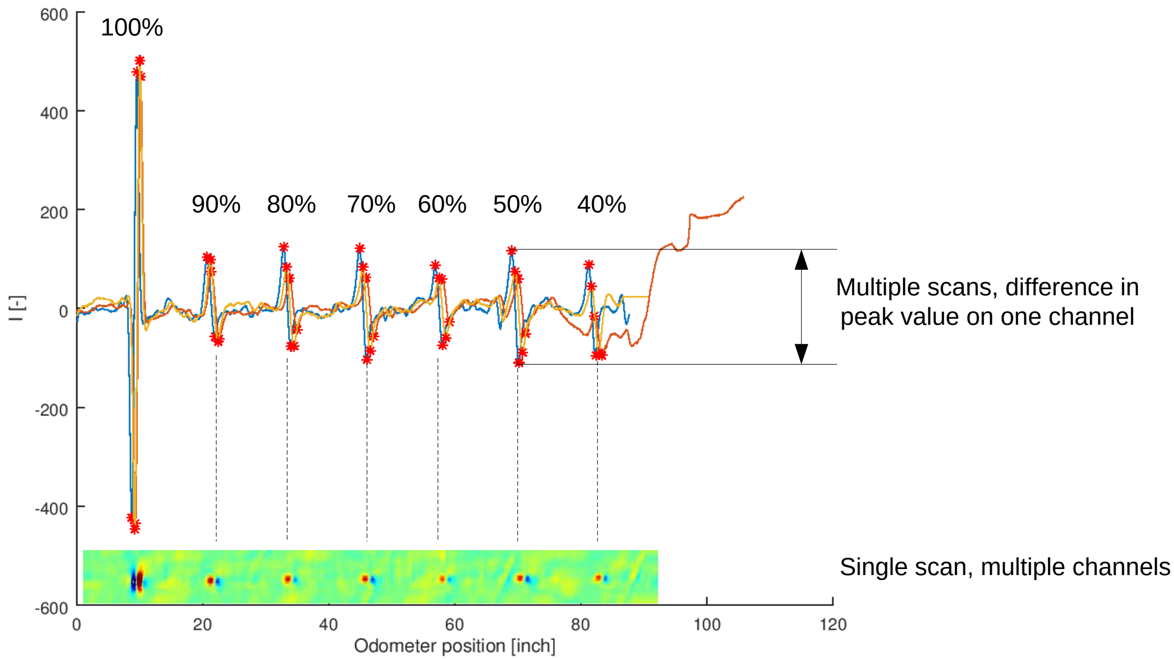

FIGURE 28: COMPARISON OF PEAK VALUES FROM PIPE WITH MACHINED SLOTS

Interference

Each AMR module contains a signal amplifier and a lock-in amplifier that is susceptible to picking up signals from adjacent sensors. Therefore, each module operates on a frequency that is shifted so that there is no cross-talk between any sensors. This means that for a complete pipe measurement, there is an effective range of frequencies used.

Task 2.3: Manufacturing of Explorer Sensor module

The centerbody and test equipment for laboratory testing was implemented in this task. The centerbody actuator and position sensor were machined and assembled. The interface with the robot was assembled and connected to the rest of the test setup. The processing electronics, signal conditioning, and power control components were installed into each of the AMR EC sensor modules received from the supplier (RMD).

Task 2.4: System Integration

Based on the test results to date, the initial approach to integration onto the 8in Explorer robot may need to be adjusted. Given that results to date indicate that magnetizing the pipe improves the detectability of the AMR sensors, it may be determined that the AMR EC sensor needs to be run after an MFL inspection. This can be accomplished by performing an AMR EC inspection immediately after an MFL inspection or concurrently by integrating the AMR EC sensor on the MFL robot. A potential integration scenario aboard the robot where the sensors can be run concurrently is shown in *Figure 29.* The AMR EC sensor and an additional support module are inserted into the MFL inspection robot, which increases the overall length and weight of the robot.

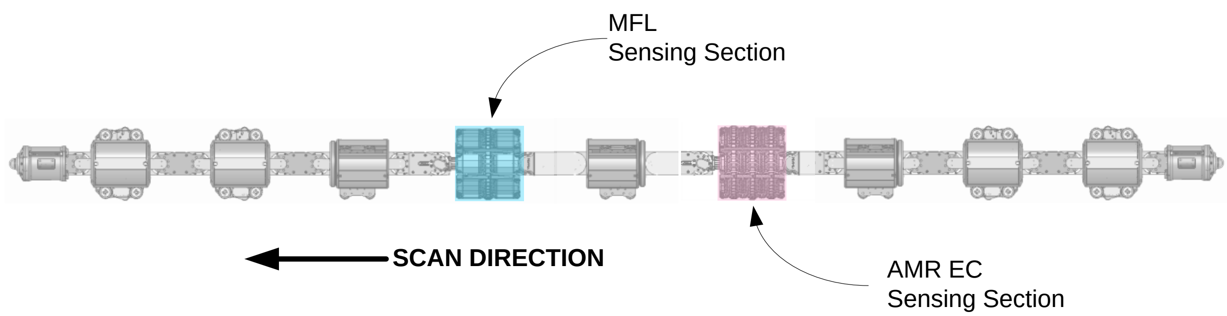

FIGURE 29: SAMPLE CONFIGURATION WITH MFL AND AMR EC SENSING

The higher signal conditioning and processing power requirements for the AMR EC sensor suite increases the overall power consumption of the robot, thus reducing the operational range (*Figure 17*). This additional power requirement is somewhat offset by the extra battery capacity offered by the added support module between the MFL and AMR EC sensing sections.

	AMR EC Only	AMR EC + MFL
Range	82%	78%

FIGURE 17: RANGE COMPARED TO MFL ONLY

Communication and control of the robot would not change from existing protocols, but the additional length of the robot does require modification of the existing pipeline entry and exit routines. Data downloads will be performed either wirelessly or through a cable connection to each nose module after a scanning run. The sensor was tested in various in-pipe scenarios including launch testing (*Figure 18*).

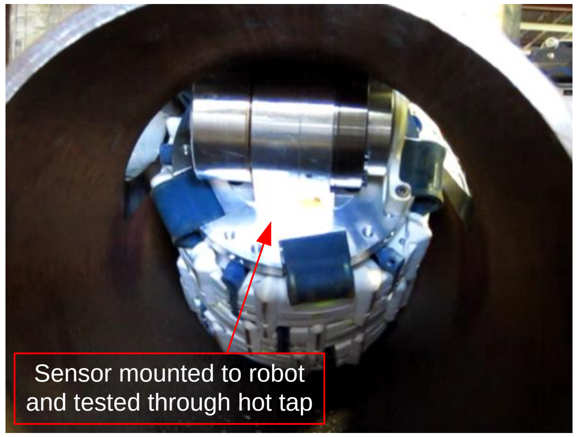

FIGURE 18: SENSOR MOUNTED TO ROBOT AND TESTED IN PIPE SCENARIOS

Task 2.5: Data Analysis Development

As mentioned during the discussion of the detailed design of the AMR sensor, a number of test samples were sourced to test the detectability of the sensor element under different conditions. Parameter sweeps were performed using a single element on this test setup. These include tests to determine the effect of sensor lift-off, driving current, frequency, magnetization, test material, speed of travel, and sensor element geometry. Analysis techniques were developed during the course of the project to evaluate the sensor performance. These steps are described in *Figure 19*.

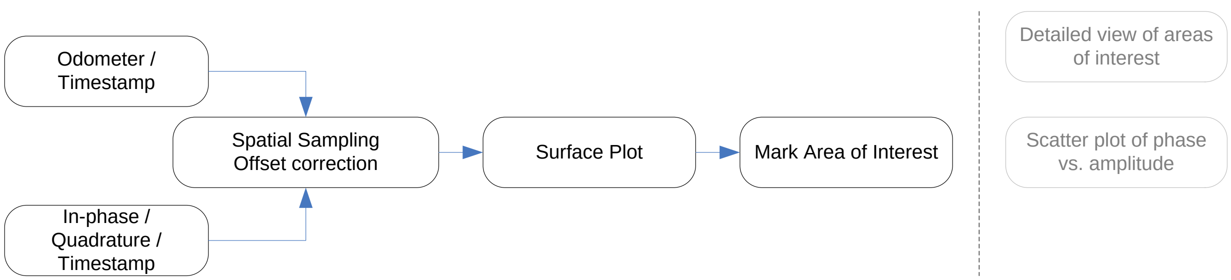

FIGURE 19: DATA ANALYSIS FLOWCHART

The data is downloaded from the AMR EC module and combined with odometer data through a spatial sampling algorithm. The spatial sampling maps the scan data to a grid of data points on the pipe. For AMR sensing this is a grid that is defined by the sampling / storage frequency of each module and the width of each of the channels (*Figure 20*).

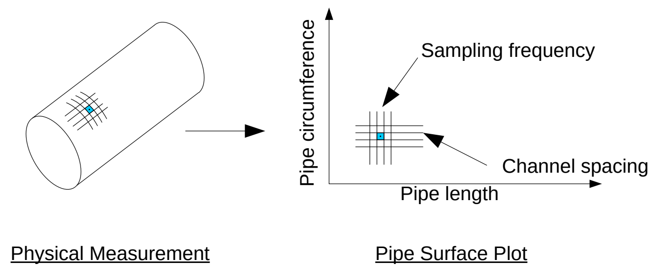

FIGURE 20: SURFACE PLOT OF DATA

After the data is mapped to a rectangular grid, it is plotted as a color map on a surface plot with the max and min values of the signal shown as a graduation between two different colors. In total, the best techniques for data analysis were limited to surface plot visualizations. Analysis of the defect data on a case by case basis was inconclusive.

Task 2.6: Pipeline Testing and Additional Laboratory Testing

The goal of this task was to deploy the system in a live transmission natural gas pipeline to test the mechanical, electronic, firmware and data collection capabilities of the system. This involved preparation and deployment to a location provided by one of the NYSEARCH member companies. Following the field testing, the robot was again tested in the laboratory on an extended data set.

Pipeline Field Trial

The robot with the sensor integrated on it was deployed in an underground transmission gas pipeline to ensure that the system could be operated under normal pipeline conditions. The test location was provided by a west coast gas company in an 8in live pipeline. The sensor was installed onto the 8in Explorer robot and deployed in a pipeline that had been previously inspected using a magnetic flux leakage sensor. The data was collected and analyzed according to the tools developed in the previous steps.

The robot was loaded into a launch chamber (*Figure 321*) and driven into the pipe. The sensor (seen in Figure 35) was deployed to the pipe wall and the eddy current exciter coils turned on. All sensors recorded the response of the AMR sensors on the pipe wall for the duration of the test. A total of 369 [ft] of pipeline was scanned with the system.

FIGURE 321 EXPLORER 8IN LAUNCH TUBE

The result of the pipeline test was a fully tested sensor system. All mechanical, electronic, and firmware systems functioned as expected. No technical issues of any kind emerged during the entire operation. All AMR sensors, coils, and sensor modules performed as in prior testing during system design and implementation. The only issue that emerged was that some plastic parts on the sensor module were damaged during entry/exit from the pipeline, without however affecting overall system performance.

FIGURE 35: AMR EC SENSOR ABOARD 8IN EXPLORER

Data was downloaded from the robot for the 369 [ft] of inspection. The data was spatially sampled and reviewed for areas of interest (*Figure 36*). The inspection did not show any indications that could be correlated back to physical defects. There were 5-10 indications consistent with material variation found during scans in the lab of defect free pipe of identical material.

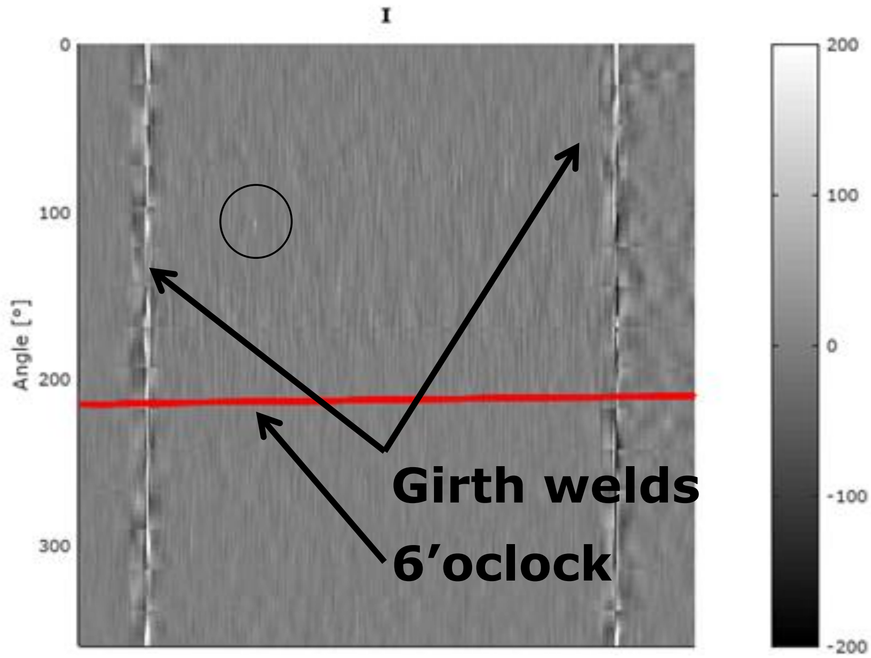

FIGURE 36: SAMPLE AMR EC DATA FROM FIELD TRIAL

Further Investigation

After the field trial additional pipes were sourced to increase the understanding of the detectability of the AMR EC system. The need to compare different types of simulated cracks was identified. A small 24in segment of pipe was sourced with four types of defects. The first was an EDM notch, the second was a thermal fatigue crack, and the third and fourth defects were mechanical fatigue cracks (proprietary method). The pipe was scanned using AMR (no magnetization). The results for this pipe are shown in *Figure*. The EDM notch is not visible, which is a similar response to the plate scan in the detailed design task. The mechanical cracks show a similar response to the cracks from Pipe #6. The thermal fatigue crack shows the same pattern, but a larger area of effect.

The second pipe was EDMed with slots from 10% to 90% along the long seam weld of the pipe. The pipe was scanned using the AMR EC Sensor and the results are shown in *Figure 38* (top). None of the notches (even the 90% notch) show up in the data. A large material anomaly can be seen at 80in and a bigger zone at 53in.

An MFL sensor was run through the pipe then the pipe was re-scanned with the AMR sensing module. The results are shown in *Figure 38* (bottom). Like in the detectability testing throughout the project, the EDM notches now show up down to 40%. The background noise is reduced as well. The large anomaly at 80in has diminished slightly as well as the 53in zone. The magnitude of the large anomaly is significantly higher than the signal from the 90% defect.

Applying an additional filter to the dataset brought out the defect signatures more clearly (*Figure*), as well as other features in the pipe. If this were a blind test, more information would be required in order to differentiate between the EDM notches and the material anomalies. This confirms the assertion that the anomalies from the live inspection are consistent with background noise of clean defect-free pipe.

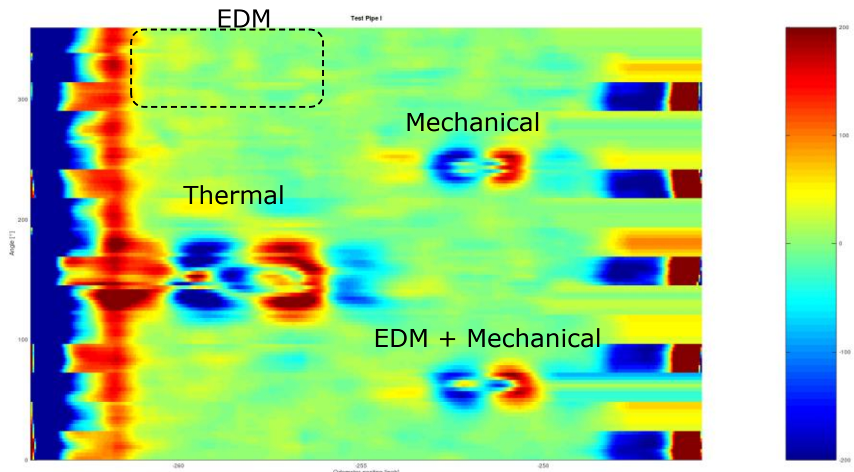

FIGURE 37: SCANS USING AMR ON A FOUR DEFECT TEST PIPE

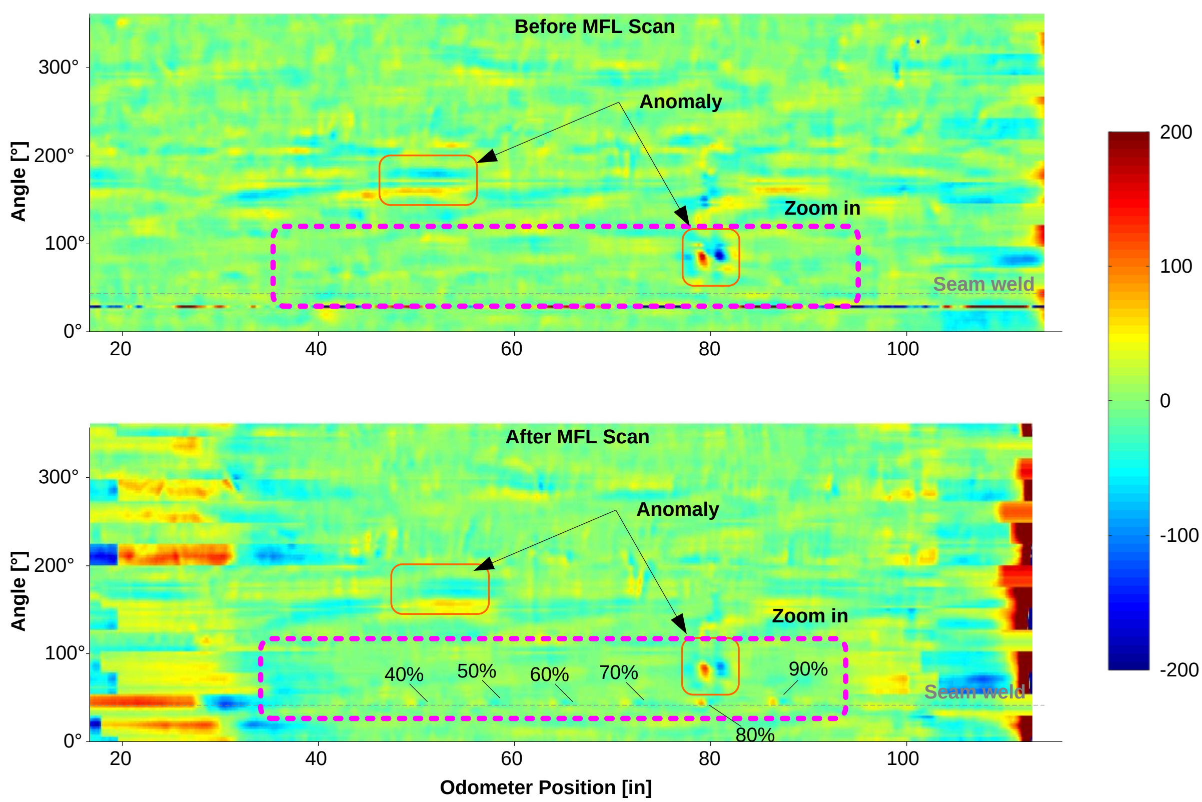

FIGURE 38: AMR EC RESULTS FROM EDM NOTCH PIPE

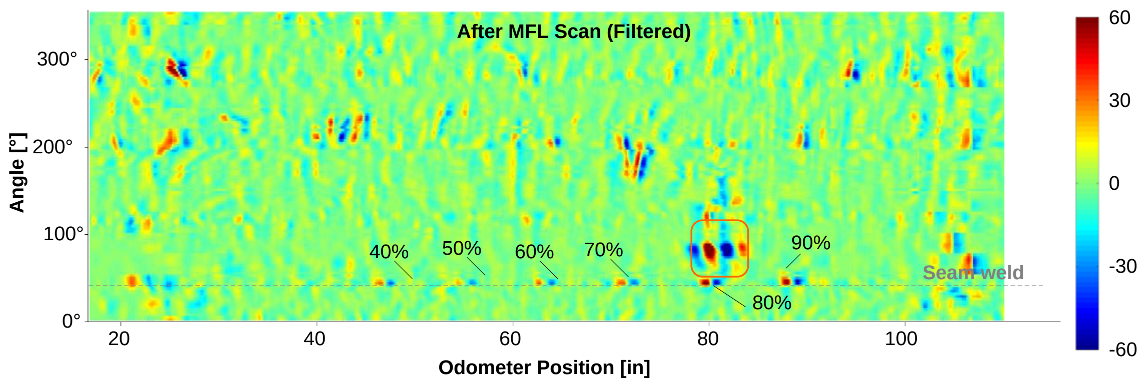

FIGURE 39: FILTERED RESULTS FROM EDM NOTCH PIPE

In summary, defects in pipes with open notches manufactured with EDM are not detectable unless there is a magnetic field applied prior to the scan. Other fatigue cracks can be detected, likely due to the manufacturing method.

The AMR EC sensor behavior looks to be affected by the stress levels in the material. Deep machined slots, non-thermal fatigue cracks, and thermal fatigue cracks all leave stress fields behind as part of the manufacturing process. EDM machining does not leave a stress field and is not detectable. Therefore, the pattern of signal for the pipe, including the anomalies, looks to be a combination of residual magnetism and stress fields from the magnetization (MFL sensor) and manufacturing methods. Table 5 summarizes the results from these tests.

TABLE 5: ADDITIONAL DEFECT SET

8in A53B 0.322WT Pipe, simulated defects			
Defect Type	**Magnetism state**	**Detected defects?**	**Other**
Non-thermal Fatigue	None	Yes	
Thermal fatigue	None	Yes	Significantly higher response than non-thermal fatigue
EDM Notch	None	No	9 defects 10%-90%
EDM Notch	Yes	Yes	9 defects 10%-90%

At this point, with all of the detectability and repeatability results, the conclusions are:

1) Any pipe in the ground that will be scanned with this sensor will have an unknown combination of material properties, stress field and residual magnetism from manufacturing, installation, and inspection processes.
2) For the AMR EC sensor to detect axially aligned cracks/slots without residual magnetism in the material, there needs to be a stress field (see simulated crack results, Task 2.2)
3) For the AMR EC sensor to detect axially aligned cracks/slots without a stress field, there needs to be residual magnetism (see EDM results above)

4) It is unknown whether the signal resulting from the non-thermal fatigue cracks (simulated) are the same as those that would be found in live pipes with cracks.
5) It is currently unknown how to differentiate between anomalies that are purely due to material property variation and anomalies that are caused by cracks forming. Identifying all anomalies as defects in the current setup would result in a large number of false positives. There may be methods of data manipulation that can be employed to separate these effects (I-Q plots), however at this time, this project has not achieved a viable approach to this problem.

An application that was considered for the AMR EC sensor was to use it to determine the position of a seam weld in a pipe. Due to its ability to repeatedly detect girth welds and variations in the material properties, in theory the sensor would be able to detect the grain structure changes associated with a the long seam weld of a pipe. A test setup was constructed to move the sensor in a circumferential direction. The data was downloaded, aligned and shows that a seam weld can be detected in this manner (*Figure 22*). This is a potential application on projects requiring seam weld positioning.

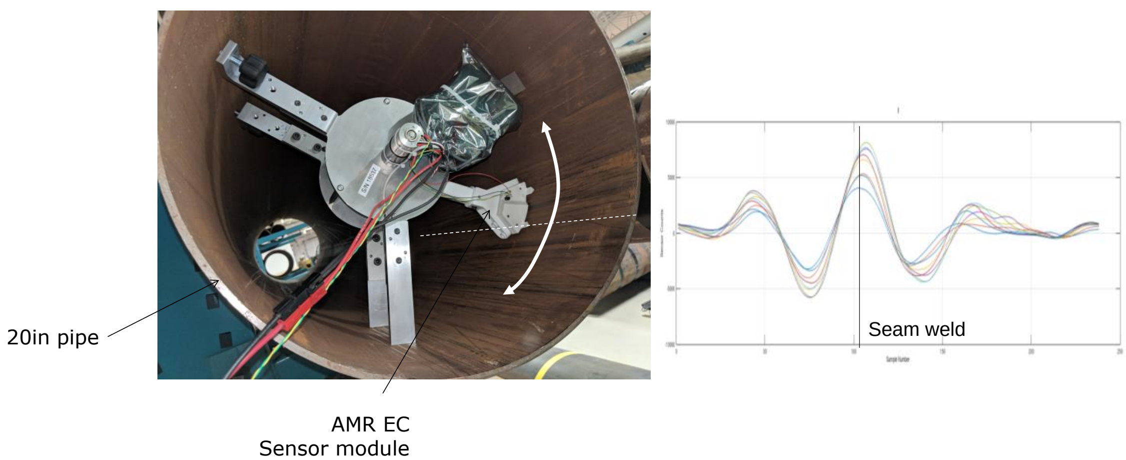

FIGURE 22: USING AMR EC MODULE FOR SEAM WELD DETECTION

Task 2.7: Project Management

Project updates and communication with various organizations involving the progress and status were tracked under this task. It also involved keeping the project on pace and making necessary adjustment to the project plan as the project evolved.

5. Conclusions

The Explorer family of robotic pipeline inspection platforms have proven their ability to provide valuable access to and data on unpiggable pipeline segments. This currently includes high resolution Magnetic Flux Leakage (MFL) data for metal loss detection, mechanical damage data as well as internal video images. As a result of recent pipeline incidents though, there is a growing desire for the addition of crack data on pipelines. While crack data can be obtained for piggable pipelines there currently is no methodology to provide that data on unpiggable pipeline segments. As such, the feasibility and prototyping of an eddy current (EC) sensor based method of crack detection using Anisotropic MagnetoResistive (AMR) sensors was performed by Radiation Monitoring Devices (RMD) of Watertown, MA. RMD's earlier work (funded by NGA) concluded that an AMR EC sensor could be implemented aboard a Pipetel Explorer 8in robot to potentially detect axially aligned cracks in unpiggable pipelines.

The objective of this project was to implement the validated sensor aboard the 8in Explorer platform and replicate test results from the first two phases in a real pipeline test setting. This involved the conceptual development, design, manufacturing, system integration and testing of a full circumference AMR EC sensor in a module format that is compatible with Explorer's 8in modular robot. In addition, data analysis capability was developed.

The validated sensor was an Anisotropic MagnetoResistive Eddy Current (AMR EC) module. InvoDane worked with the sensor supplier to determine a mechanical arrangement that would allow the sensor to be mounted to Explorer. In the end, 15 units were mounted in a collapsible assembly for full coverage of the pipe wall.

InvoDane developed the signal processing hardware and software to collect the eddy current data and store it for download from Explorer after an inspection run. The data sampling and onboard filtering were validated against laboratory equipment successfully.

During detectability and repeatability testing, it was found that pipe samples used to validate the sensor had defects that were constructed in a manner that left large stress fields and grain structure changes. During detectability testing it was found that even the smallest of defects (10%) could be found which was unexpected. The team demonstrated that the sensor could detect small defects if there was a stress field (no magnetism). The team also demonstrated that medium sized defects were detectable (40% and greater) if there was a residual magnetic field present (no stress).

For an unpressurized pipe sample with naturally occurring cracks, the AMR EC sensor was not able to detect a majority of the cracks in a seam weld. It is assumed that this is because the stress field has changed since the cracks were formed under pressure but this has not been validated.

The AMR modules were tested in order to develop a sizing approach. The repeatability of the sensor from run to run was consistent; however the levels of each channel compared to each other were not. Attempts to calibrate the sensor resulted in improvements to the sensor construction, namely alignment of the AMR channels and securing them with epoxy. A sizing approach was not possible since the best calibration of the unit resulted in an error of approximately 15-20%. The sensor was supplied as-is with an amplifier and signal conditioning board in two sets of 15 modules.

The mechanical chassis of the centerbody that connects the 15 modules was constructed and connected to the test setup in the laboratory. The 15 modules were assembled and arrayed around the centerbody. Interference tests showed that all sensors needed to operate on a separate frequency. The test setup was used to scan 8in pipes in the lab.

The AMR EC Sensor (centerbody + 15 modules) was installed on an Explorer robot and live tested in August 2018. Results from the test were consistent with background levels in pipe from laboratory scans.

Further tests were conducted after the live field trial. The team did tests on defects made with zero stress and found that these were not detectable with the AMR EC sensor. After magnetization, the defects could be detected, but only at the same level or lower than other anomalies due to material variation in the rest of the pipe.

In summary, the project resulted in a setup that could reliably produce results that showed a combination of magnetic and material properties of a pipe. The team showed that the sensor could detect defects with zero stress as long as there was a residual magnetic field. The team also showed that the sensor could detect defects with a stress field if there was no magnetic field. The team could not differentiate between the effects of all three (material properties, residual magnetism, stress field) in a single data set.

6. Acknowledgements

The support of PHMSA/USDoT in cofunding this effort is acknowledged. NGA and Invodane Engineering would like to acknowledge and thank PHMSA for its continued support of R&D efforts to develop and expand the capabilities of the Explorer family of robots over many years. In addition we would like to thank the natural gas industry for its continued support in providing access to its infrastructure for field tests.

APPENDIX A

NONDESTRUCTIVE INSPECTION (NDI) OF PIPES USING AMR SENSORS FOR ECT

Final Report

TASKS 1.1 to 1.4

Radiation Monitoring Devices, Inc.

NONDESTRUCTIVE INSPECTION (NDI) OF PIPES USING AMR SENSORS FOR ECT

Final Report

PUBLIC

Radiation Monitoring Devices, Inc.

44 Hunt Street

Watertown, MA 02472

Report Prepared for NYSEARCH/NGA

April 30, 2018

1. EXECUTIVE SUMMARY

In the program sponsored by NYSEARCH/NGA, RMD is capitalizing on the unique performance features of its anisotropic magnetoresistive (AMR) sensors to create and demonstrate prototype Eddy Current Test (ECT) probes developed specifically for the challenges of gas pipeline inspection. RMD has tested several traceable standard pipe samples and successfully detected most of the representative flaws. Significant challenges during the research work were discovered and investigated. These most significantly included the effect of anomalies in the material that had significantly larger response as compared to the target flaws. Unexpectedly, very deep flaws that pose difficulty for electromagnetic inspection often showed significant response with the sensor probes.

During the development, we implemented new concepts using the AMR sensor to detect flaws in thick gas pipe walls, based on our research work developing the sensor concept for this application. This sensor module uses eddy current technology to detect axial cracks in pipelines. The advantages of this system are its light weight, low power consumption, and capability to be mounted in a small, directionally oriented module to match the contour of the pipe wall. A lighter NDE system would extend the range of battery powered robotic Explorer systems (developed by InvoDane Engineering) used for NDE, saving time and money during in-line inspections.

In earlier work, not funded through this program, RMD studied and demonstrated the applicability of the AMR-based eddy current probe's effectiveness in pipe wall inspection. RMD also developed a robotic scanning mechanism to enable us to scan long distances without changing the setup so that it is possible to accurately compare the response of the ECT probe to multiple defects along a single path. This scanning mechanism was used in conjunction with our prototype to scan a variety of defects on additional pipe samples. After acquiring additional pipe samples, RMD was able to detect most representative flaws with a high confidence using our prototype Magnetoresistive Eddy Current (MREC) modules. We began working with InvoDane Engineering on the concept, pipe scans and probe testing.

In this project, RMD continued working with InvoDane Engineering to integrate our eddy current array sensor into a field test prototype that can be used in gas pipeline inspection. We investigated methods to increase signal to noise, including degaussing, eliminating cross coil interference and sensor alignment. Along with these techniques, we designed and assembled 4 Prototype versions, with each improving upon the last in some significant way. We established a calibration procedure that is effective at reducing both sensor-to-sensor and module-to-module variation. We concluded our work with the delivery of 30 MREC Prototype Version 4 probe subassemblies to InvoDane.

2. TECHNICAL OBJECTIVES

The technical objectives of this workscope are to:

- Build 8 Channel MREC Prototype
  - Custom molded body
  - Coil Driver
  - 8 AMR Sensor design
- Test on representative samples
  - Low Carbon steel plates and half-pipes
  - 20 Inch pipe from FlawTech
- Miniaturize Support Electronics
- Confirm performance
- Integrate into Explorer platform
- Field Test

3. NEW RESULTS AND INSIGHTS

Material anomalies

Through extensive experimentation, it has become apparent that the magnetic sensors used in the MREC modules are sensitive to magnetic perturbations in the steel pipe walls, which could come from the manufacturing process, material variation in the grain structure, or the magnetic condition remaining after other in-line inspections. If the pipe magnetic material state is unknown, which is the case in most installed pipelines, then responses due to indications of magnetic anomalies must be filtered out. We have found that axial flaws, which are specifically targeted with the design of the MREC module, have a distinct characteristic signature. This information may be able to be used to help differentiate flaws from anomalies.

Some pre-test uniformity can be achieved if the MREC system scan is preceded by a 'conditioning' scan that consists of a large uniform flux applied to the pipe wall. This would need to be designed to put the pipe in a known magnetic condition, assuming enough energy is applied to affect the entire through-wall thickness. An operation that applies a large magnetic flux, such as MFL testing can produce a significant degree of uniformity in the metal. This can also accentuate the flaw response by leaving residual magnetization around breaks in the material (such as fatigue cracks), of which the MREC modules are greatly sensitive to. This direction of work requires further research.

Unexpected responses from deep flaws

Eddy currents have a fundamental depth limit, defined and measured by the skin depth. This is the depth at which electromagnetic currents protrude into the surface of the material, and it depends on the material conductivity and permeability. Some flaws were estimated to be deep enough so that only a tiny fraction of the eddy currents will reach them, making it unlikely that they could be seen with the probe. During our research, RMD and InvoDane discovered that flaws that should otherwise be too deep to be detectable by eddy current were indeed showing indication with the prototype system developed here. There could be two explanations to this phenomenon. The most likely is that the flaws due to thermal cycle fatigue or stress fracture could release residual stress from pipe-forming operations in the surrounding material, far through the wall. It may be this change in stress condition in the middle or near the inner surface results in the flaw indication from the eddy current module. Theoretically, at a depth of ¼" or more (depending

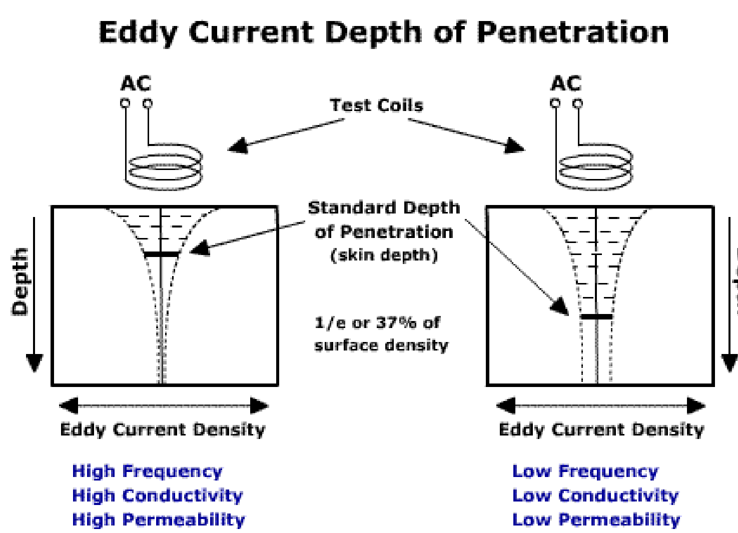

FIGURE 23: DEPTH OF PENETRATION (COURTESY OF NDE-ED.ORG)

upon material properties), the eddy currents are reduced to a tiny fraction of the currents at the surface[2], making direct eddy current inspection result in very low SNR (signal to noise ratio) signals for deep flaws with no other material variation. This is illustrated in Figure 1. Eddy current inspection is sensitive to material stress condition, so this stress change when a crack occurs is likely a cause[3,4,5].

The second possibility is that during fabrication of the pipe, magnetic gradients are present in the material. This is dependent on how the material was manufactured[6,7]. When cracks form, the magnetic domain potential across domain grain boundaries change in some way, resulting in embedded magnetic anomalies in the wall. Either of these scenarios and others are possible, but investigation into these issues requires further research.

Other explanations are possible, but those are yet to be discovered and explored.

Sizing

Sizing becomes very difficult because it is very challenging to differentiate the unknown effect of magnetic anomalies in the material or anomalies introduced by other means, from the pure (true) flaw response. To some degree, length can easily be determined for very long flaws. Clear indications of axial flaw beginning and end, as the scan is performed, can be used to measure length. Depth of flaws should be measureable by varying the eddy current frequency, and looking at the change of response, including phase of the signal. As eddy currents are perturbed by flaws at deeper depths, the phase of the response shifts. This is useful in non-magnetic materials, because the specific magnetic condition of the material does not vary. In magnetic steel pipes, this is a significant challenge that needs to be investigated.

Calibration

We have developed a method of calibration that normalizes the response from each of the sensors in the MREC module, such that minute variations in the construction of the coil, and the direct coupling of the sensors and leads are cancelled out. This is based on the understanding that the response from a highly uniform, controlled discontinuity is repeatable across different types of scans over many materials. The purpose is to make the measurements from sensor to sensor and module to module all be equivalent. In order to use calibration to accurately size the flaws, an exact representation of the material as part of the calibration setup is required. This would require more investigation and a guarantee of the pipe material under test. More details of the calibration procedure and results are below.

---

[2] https://www.nde-ed.org /EducationResources/CommunityCollege/EddyCurrents/Physics/depthcurrentdensity.htm

[3] M. Zergoug, G.Kamel, N.Boucherou "Mechanical Stress Analysis by Eddy Current Method", ECNDT, Berlin, 2006

[4] Dahia A, Berthelot E, Le Bihan Y, Daniel L. "A model-based method for the characterization of stress in magnetic materials using eddy current non-destructive evaluation." Journal of Physics D-Applied Physics. 2015; 48(19).

[5] Tian, G.Y.; Zhao, Z.X.; Baines, R.W. "The research of inhomogeneity in eddy current sensors" Sens. Actuat. A 1998, 69, 148-151.

[6] Siebert R, Schneider J and Beyer E. "Manufacturing Related Effects on Magnetic Properties of Electrical Steels." ***6th International Conference on Magnetism and Metallurgy WMM'14***, 2014.

[7] Schoppa, A.; Schneider, J.; Wuppermann, C.-D. "Influence of the manufacturing process on the magnetic properties of non-oriented electrical steels" Journal of Magnetism and Magnetic Materials, vol. 215-216, issue 1, pp. 74-78.

Material Differences

Pipes manufactured with different specifications and materials, will likely have small differences in their magnetic properties, specifically permeability[8]. Typical variations in permeability has a much larger effect on eddy current and depth of penetration than typical conductivity variations. This can cause the flaw response in one pipe to be distinctly different than an identical flaw in another pipe of a different material. It was not possible to directly compare a thermal fatigue crack in our pipe samples to another pipe material, because no two manufactured flaws are the same. More of this research is recommended to understand specifically how material makeup relates to magnetizing and anomalies as already discussed and as discussed in the recommendations.

[8] Schoppa, A.; Schneider, J.; Wuppermann, C.-D. "Influence of the manufacturing process on the magnetic properties of non-oriented electrical steels" Journal of Magnetism and Magnetic Materials, vol. 215-216, issue 1, pp. 74-78.

4. BUILDING ON EARLIER WORK

The following is a summary of the work performed in the earlier work (prior to initiation of the workscope of this project) that was relevant to the work carried out for this project.

Baseline Scans of Pipe #1 for reference

In the earlier work of the development program[9], we took several baseline scans of Pipe #1 (20” A672 ¼” wall with 1” axial flaws) with both our fine pitch X/Y scanning system as well as our single pass, whole length scanner. We used these baseline scans to define control areas of the pipe as well as determine how each representative flaw looked compared to that control. Each set of flaws is clearly differentiated from the control scan. The flaws ranged from 10% - 50% through ¼” wall, including both ID and OD cracks. The result of this work was the basis for the confidence that we had in the performance of the sensor system.

Magnetization of Pipe #1 flaws

Of concern was the possibility of false positives caused by anomalies in the steel wall, including residual remnant magnetic flux (magnetization). From our early investigations and modeling, it was clear that soft magnetic materials can retain remnant flux that can affect how the eddy currents penetrate the pipe wall. We wanted to experiment with this phenomenon and judge whether these anomalies can be significant causes of false positives.

We then placed strong rare-earth magnets at various places along the outside and inside of the pipe to determine what, if any, effect this would have on the sensor. We scanned over both Flaw 6 and the area where the magnet had been placed, which was offset both axially and circumferentially from the flaw.

The characteristic shape of the axial flaw using our AMR based eddy current module is identifiable, and this experiment showed that magnetic anomalies in otherwise nominal wall sections are distinctly different. A number of anomalies were investigated. Our initial conclusions led us to believe that discerning these anomalies was possible during inspection.

Design and Build first MREC Prototype probe

The first MREC Prototype (V1) consisted of 6 AMR sensors. It contained no support electronics within the body of the probe, and bench top coil drive and pre-amp.

This generalized shape was selected to fit a fractional slice of a pipe section, and the concept of embedding the sensors and interconnects began with this prototype.

Test MREC Prototype probe

REC V1 was then used to scan Pipe #1. It showed promising, repeatable results that matched the baseline. We were also able to compare the signatures of multiple sensors to show that sensor placement in relation to the coil edge was not significant.

[9] “NONDESTRUCTIVE INSPECTION (NDI) OF PIPES USING AMR SENSORS FOR ECT”, PHASE II FINAL REPORT, FEBRUARY 5, 2015.

5. COMPLETED WORK IN THIS PROJECT

The following is a detailed summary of the work performed in this project.

Prototype circuitry development

Figure 2 shows the initial prototype circuitry for the coil drive and pre-amp. These were based off of similar circuits used in other eddy current research projects.

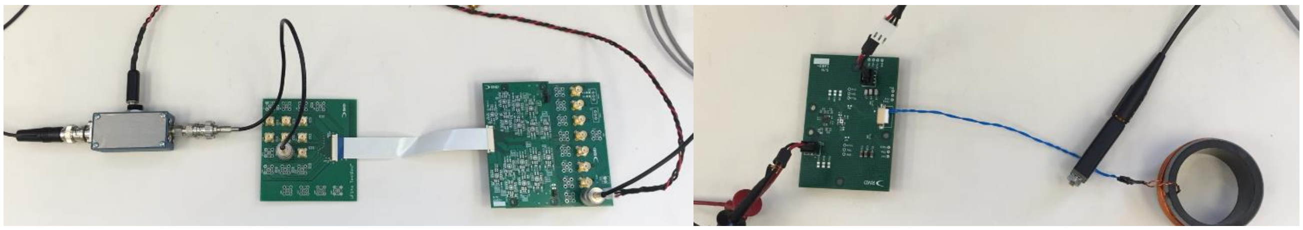

FIGURE 2: PROTOTYPE CIRCUIT FOR INITIAL MODULE TESTING.

Pressure Test Components

InvoDane performed pressure testing on the electronic components to confirm their ability to function in a gas pipeline under pressure. Both the prototype sensor electronics circuit and the coil electronics circuit were tested and passed inspection. The pressure test set-up, located at InvoDane Engineering, can be seen in Figure 3.

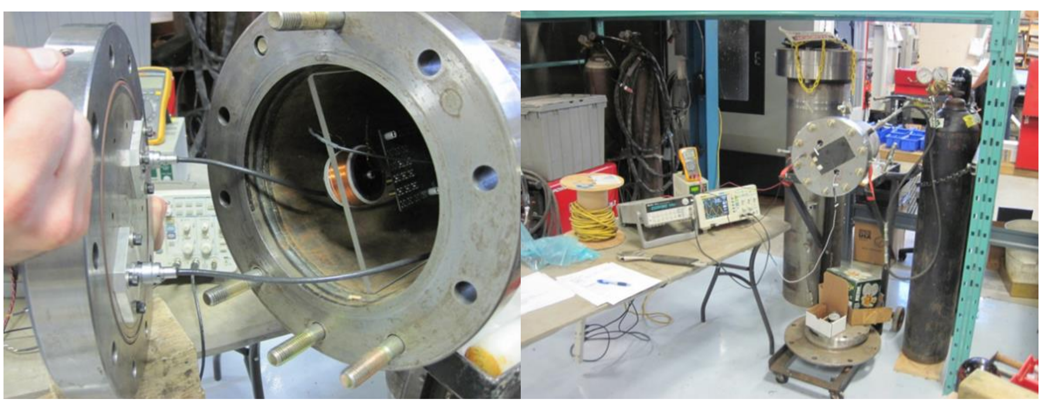

FIGURE 3. PRESSURE TEST PERFORMED AT INVODANE ENGINEERING.

Coil Design

The MREC module is surrounded by the drive coil, which induces the necessary eddy currents in the pipe wall. Perturbations in the electromagnetic fields are then picked up by the sensors that are in closest proximity. In order to maximize the field generating capability, the coil is designed to follow the exterior contour of the section volume of the MREC module.

The design goal of minimal size led to the requirement that much of the support circuitry be contained within the module. This required that careful attention be paid to the circuit design and how these driving fields will affect the performance of the pre-amp and the stability of the drive circuit.

Sensor construction and placement

The AMR sensors are produced by RMD in several ways. For research activities and early experimental design, our partner fabricators produce die-level AMR sensors to RMD's specifications. With die-level sensors, many extremely tight and geometrically controlled configurations can be built, for instance by arranging the sensors into tight sub-millimeter arrays for fine pitched, high resolution scanning. AMRs are fabricated on a substrate, with magnetoresistive strip. A diced wafer of single AMR stripe sensors is shown in Figure 4 (left), and several AMRs of varying configurations are shown in the center.

Alternatively, and for production of highly reliable, mechanically robust sensing systems, the entire AMR sensor is produced and packaged by an outside manufacturing vendor. This is done where the design can accommodate standard device packaging, and wire-bonded, leaded, and encased packaging is required for reliable operation. A packaged and assembled AMR sensor is shown in Figure 4 (right).

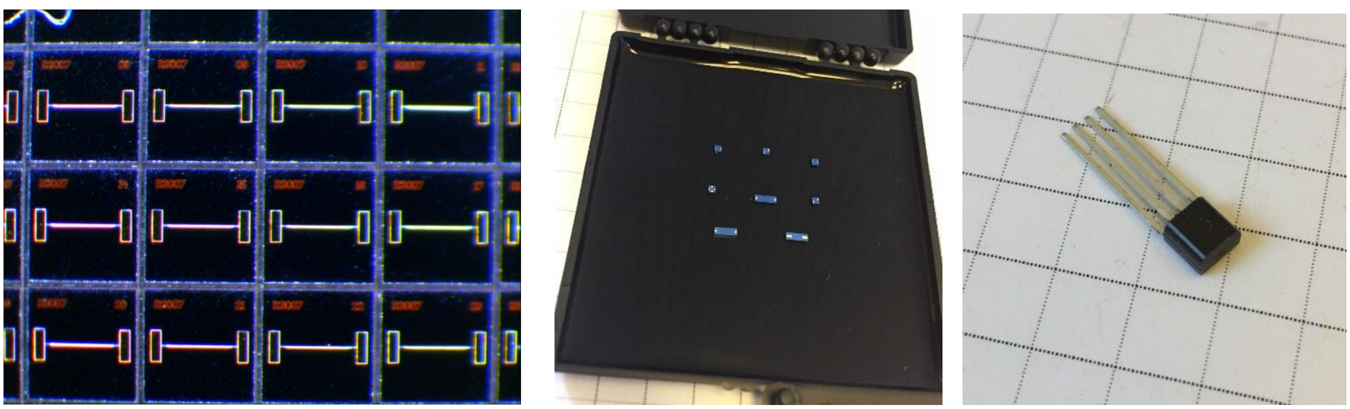

FIGURE 4: SINGLE SENSOR AMR DICED WAFER (LEFT). VARIOUS RMD MR SENSORS (CENTER). STANDARD PACKAGED AMR (RIGHT).

Design and build second MREC prototype probe

The second MREC Prototype (V2) consisted of 8 AMR sensors. It contained no support electronics within the body of the probe. It did, however, have the coil drive circuit located outside of the coil area (on the "back" of the probe), and a prototype eight channel pre-amp circuit between the module and the eddy current inspection instrument. The body of this version was based on the final design as specified by RMD and InvoDane.

This version was used in testing that verified the selected positioning and spacing between sensors. The coil geometry was preliminarily specified and verified with this prototype. With a fully defined coil structure, the design of the coil driver circuit could be finalized. This version also had skids, which provided consistent spacing to the pipe wall. This version was also built to match the internal diameter of the 8" pipe and the proposed collapsing shape and mounting in the Explorer robotic platform.

Circuit Architecture

The MREC electronics were split into distinct subsections. RMD developed the sensor board with pre-amp, which converted the differential signal from the sensors to an amplified output. RMD also developed the coil drive electronics. InvoDane Engineering designed the analog conditioning component and the digital processing board. This DSP functionality replicates the instrument setup for eddy current testing at RMD.

Design and build of the drive circuitry

To drive the coil current, a signal of nominal power needed to be amplified. This circuit is optimized for power. This circuit was designed in the shape of the MREC module frame. Testing included verifying that the circuit could operate without adverse effects in such close proximity to the driving field generated by the coil.

Design and build of the sensor pre-amp

The sensors require power and amplification as close as possible to the sensors to minimize injection of unwanted noise and direct coupling from the coil. Some of this is inevitable, but with a near-sensor amplifier, much of this can be mitigated. The pre-amp is designed to amplify the sensor signals and interface to a control board. It also acts as a pass through for power and signal to the coil driver.

Design and build third MREC prototype probe.

The third, MREC Prototype (V3) consists of 8 AMR sensors also. The body of this version was based on the final design as specified by RMD and InvoDane. This version contained the drive printed circuit board (PCB) and pre-amp PCB. Two versions were made, including an 8" pipe version and a flat plate version.

Design and build fourth MREC prototype probe

The final design produced was Version 4. This version incorporates mounts and space for signal conditioning and contral boards from InvoDane. Information and specifications about the final configuration are included in the design documentation. This includes sensor spacing, board sizes, power requirements, communication protocols, and interfaces with InvoDane components.

Flat Plate Testing

To evaluate the performance of the sensor module, a flat plate version was built. The intent with the development of the flat plate probe, was to more easily study the performance of the sensors by simplifying the scanning complexity of a curved pipe surface. Creating benchmark scan samples and crack samples in plates is much less costly and x/y scans are more straightforward to study.

This module consisted of the same electronics and sensors that were contained in the Version 3 prototype, except that the sensors were arranged in a flat line.

We used our large Epson 3-Stage Scanning Robot to scan plates with the Flat Plate MREC module (Figure 5).

Invodane sent their plate for testing to us in order to verify their results. This plate is 24” by 24” by .25” thick. It has two large notches measuring 1.5” long by 1/16” wide with 50% through depth.

FIGURE 5. EPSON 3-STAGE SCANNING ROBOT WITH FLAT PLATE MREC.

Multiplexing sensor array scans

We tested the full module functionality on a flat plate by operating all eight channels in a single module simultaneously through a multi-channel ECT instrument. Each of the sensors should have approximately the same sensitivity, and we performed these scans with no calibration. The results of one scan over a pipe flaw show that the flaw can be seen equally by each sensor, with very slight differences due to the sensors not being calibrated.

Contending with Residual Magnetic Interference in the Flat Plate.

The Flat Plate sample from InvoDane showed significant magnetic variations when scanned with the MREC module. Using a magnet, we were able to “smooth out” the magnetic signature from the plate while maintaing a clear defect signature. The results of this process can be seen in Figure 6. Flaw signatures are usually distinct.

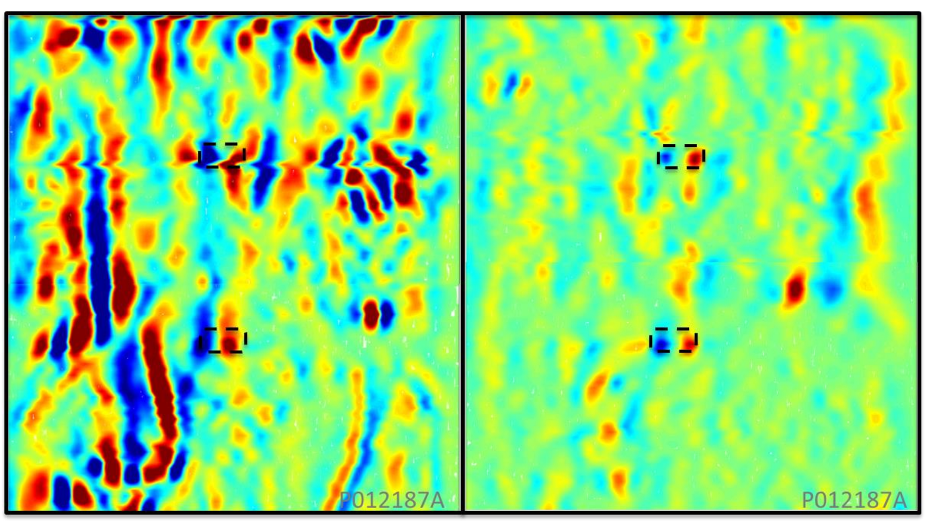

FIGURE 6. (LEFT) FLAT PLATE BEFORE “SMOOTHING”. (RIGHT) FLAT PLATE AFTER “SMOOTHING”. DEFECTS ARE HIGHLIGHTED WITH DASHED BLACK BOXES.

Potential Cross Coil Interference

In the proposed Explorer crawler configuration, 15 MREC modules will be in close proximity to each other, with any given module having as many as 6 close neighbors. There could be cross talk or interference between adjacent modules. Choosing the design points of each module carefully, we were able to eliminate this problem.

Degaussing

While the initial "smoothing" process greatly increased our signal to noise ratio, it still left potential false positives in the plate. We developed a process to completely eliminate this magnetic interference in the plate via degaussing. The apparatus is shown in Figure 7**.**

We discovered that with a thorough degaussing, we were able to remove or greatly decrease the affect of magnetic anomalies in the signal and increase the signal to noise ratio. We also discovered that magnetic anomalies can easily be introduced into the material, and depending on their orientation and strength, these responses could be significantly greater than the response of any test flaw.

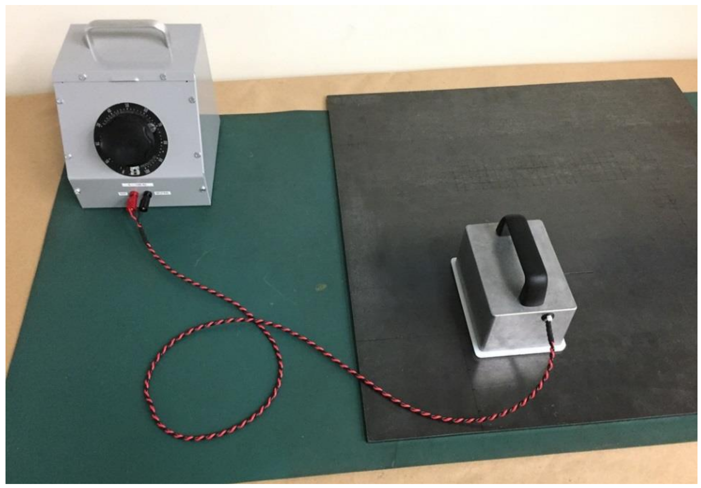

FIGURE 7: APPARATUS TO DE-MAGNETIZE STEEL PLATE AND PIPE SAMPLES

Calibration

We developed two different forms of calibration for the MREC modules. The first was designed as a functional verification and calibration of the individual sensor sensitivity and pre-amp gain. Regardless of the EC drive field and orientation and characteristics of any flaw, the individual sensors have a specific sensitivity that can vary slightly from device to device. In addition, there are small differences in the amplifier gain of each channel that must be considered. There is a uniform electromagnetic field generated and applied to each of the eight sensors. The fixture is plastic and a controlled coil construction guarantees as uniform as possible field is incident on all of the sensors.

This fixture creates a uniform field on the sensor array that can be measured and used for gain and phase response calibration. A second fixture is designed to test the entire analog sensor front end (including the sensor sensitivity, lead inductance, and pre-amplifier gain and phase response) and is used to calibrate the module assembly against a benchmark notch.

The module calibration uses a uniform, highly predictable, anomaly-free block with a controlled gap. The MREC module swings uniformly across the gap, providing the exact same conditions for each sensor. The calibration scan is done this way so that each sensor is exposed to exactly the same material break position as its neighbor.

We set up a calibration procedure in order to minimize sensor to sensor and module to module variation. It allowed for consistent, highly repeatable calibration scans. Magnitude and phase calibration factors were generated and stored for each MREC module serial number. We then scanned defects in two different pipe materials.

The measurements from the calibration block on each sensor are recorded and are applied in post processing of the scan data. The results from calibration were very promising as we were able to significantly reduce sensor to sensor and module to module variation.

6. INTEGRATION INTO ROBOTIC PLATFORM AND FIELD TESTS

InvoDane Engineering has integrated the MREC modules into a 3 x 5 cylindrical scanning body as part of a new Explorer platform pipeline inspection prototype. This system has been used to test various pipe sections that contain known flaws. This work also highlighted the need to better understand magnetic anomalies and stress induced effects of flaws in manufactured pipe and flaw formation.

7. SUMMARY OF PROJECT ACTIVITIES

Finalize design based on Phase II results

The design of the MREC module was completed to enable fully embedded prototype testing of the modules built into the eddy current array module on the robotic platform. This consisted of the pre-amp and coil drive board, as well as the mechanical design of the module frame and coil holder. RMD worked with InvoDane Engineering to complete the module architecture. Details are included in the design documentation.

Fabricate 16 modules based on final design specifications

Two batches of 15 MREC modules each were eventually built to the latest revision. The mechanical structure was fabricated using a robust nylon material. Circuits were fabricated, assembled and tested. All assemblies were built and all MREC modules were calibrated. Each module has serial number tracking.

Test and deliver 16 modules

All modules were tested and calibration data was provided to InvoDane for test and analysis. The first set of 15 MREC V4 Modules was delivered o InvoDane Engineering on October 19, 2017. The second set of 15 MREC V4 Modules was delivered on January 26, 2018. (Figure).

FIGURE 8. 15 MODULES PACKAGED FOR DELIVERY.

8. RECOMMENDED FURTHER RESEARCH & NEXT STEPS

We would recommend further research into the effects and advantages of using magnetic conditioning to pre-set the magnetic state of the pipe wall. Work would include investigations into the metallurgy, forming processes, and treatment to understand how pipe steel varies in the manufacturing process and how permeability varies. Pre-conditioning could reduce the variability in the magnetic anomalies in and around flaws. We would also study how magnetically saturating the material affects uniformity of measurement. Pre-conditioning the magnetization of the metal wall could provide a method of enhancement of discontinuities in the pipe wall. Research into the applicability of this method is needed. The possible goal of this would be to explore how well applied flux can be used to magnetize the wall around a flaw and how that would accentuate the flaw response.

Further experimentation is required to investigate methods to differentiate flaws from material anomalies, to measure probability of detection (POD) and determine sizing capability.

More work is needed to study the in-crawler performance, including crosstalk between modules.

Improvements to the MREC module could be implemented in further work. This includes the coil current monitor, some mechanical design improvements, and changes to the board connection to make assembly more reliable and simple.